THE ABSOLUTE COSMIC-RAY IONIZATION IN THE ATMOSPHERE AT BALLOON ALTITUDES

Thesis by

Alan Robert Johnston

In Partial Fulfillment of the Requirements

For the Degree of

Doctor of Philosophy

California Institute of Technology

Pasadena, California

1956

ACKNOWLEDGMENTS

The author wishes to express his thanks to Dr. H. V. Neher, under whose supervision this work was performed. His numerous suggestions and constant help throughout the period of the research were greatly appreciated.

It is also a pleasure to acknowledge the help of Dr. E. W. Cowan, who gave valuable assistance during the last six months of the work, when Dr. Neher was away.

Thanks are also due to Mr. Emil Boblett, who made the two standard condensors.

Finally, it is a pleasure to acknowledge the support of the joint program of the Atomic Energy Commission and the Office of Naval Research.

ABSTRACT

A determination of absolute cosmic-ray ionization at balloon altitudes has been made using an integrating ionization chamber. It was filled to 1 atm with argon, and was calibrated to give ionization in the argon.

The ionization produced by nuclear particles in 5 charge groups, electrons, μ's, and stars was computed between 10 and 140 gm cm^{-2} to form a basis for estimating the wall effect and recombination.

The important corrections for wall effect were from stars and low-energy electrons. A $1.4 \pm 1.7\%$ effect was estimated, the ionization being less without the wall.

Recombination was investigated and found negligible in the 1-atm chamber.

The resulting ionization in argon was converted to ionization in air on the basis of the relative ionization by charged particles in the two gases. The relative ionization of 340-Mev protons, from cyclotron experiments, was corrected by energy loss theory to give the relative ionization of particles with cosmic-ray velocities.

The final result was that ionization values obtained with the existing calibration should be multiplied by 1.049 ± 0.031 to obtain the correct ionization, from 7 - 140 gm cm^{-2} depth. The unit used is ions cm^{-3} sec^{-1} atm^{-1} of air at $20^{\circ}C$.

Further experiments were suggested.

TABLE OF CONTENTS

I. INTRODUCTION

A. Historical

Integrating ionization chambers have been used by many workers (1,2,3,4) to measure cosmic-ray intensity, and are a rather convenient and accurate tool to compare radiation existing at different altitudes, latitudes, and times. However, in cases where absolute ionizations are quoted, comparisons between values of different groups are considerably less reliable than if measurements based on the same calibration are compared. Usually, the relative measurement is the main objective.

Measurements of ionization are more significant than as merely relative ones, because ionization is related to both energy lost in the atmosphere, and particle flux. Each ion pair represents the loss of a definite amount of energy by some ionizing particle. Neglecting neutrino loss, the total number of ion pairs formed in a column of unit cross section in the atmosphere is proportional to the total energy passing through a unit area from the top of the atmosphere. Particle flux can also be computed if the specific ionization is known, since $I = J\sigma$. These relationships can be no more accurate than the absolute ionization.

Other methods are available to measure the total energy flux of the primary cosmic radiation. First, the particle

flux can be measured above the atmosphere by rocket-borne counters (5). Using the average particle energy derived from geomagnetic considerations, the total energy flux can be computed. Secondly, a detailed accounting can be made of the energy dissipated in the atmosphere by all known processes (6,7). In the past, these three methods have not shown satisfactory agreement, with ionization chamber data tending to be about half the rocket counter data. Reasons for the difference were known to exist, since neutrino loss and recombination make ionization chambers read low, and albedo makes the rocket results high. A recent paper by Meredith (5) has indicated that albedo is the big effect, but it is still desirable to check ionization values.

An extended series of measurements of cosmic-ray ionization at high altitudes has been made by H. V. Neher (3,8,9). These measurements were made with one type of ionization chamber, intercompared by the same procedure from flight to flight, and year to year. The accuracy of the intercomparison was quite good, being somewhat better than one percent. However, the normalization used has been carried along from a calibration made in 1931. Different fillings, sizes and well thicknesses have been used in the past. The absolute calibration is therefore considerably more uncertain.

For these reasons, it was felt desirable to make a new determination of the absolute ionization which would apply to Neher's chambers.

Neher's telemetering chambers are described adequately in the literature (10). The ionization standard is maintained by a number of such chambers selected for their consistency of operation. If one of these should become erratic, there are always several others to point out the guilty one. The intercomparisons are made using a Th C" gamma-ray source, which is shielded by 1 cm of lead. A set-up is provided that enables any of the instruments to be placed in the same position, at the same distance from the source.

Just before a flight, the instrument to be sent up is placed in the set-up, and its response obtained with the known gamma-ray ionization. The level of ionization used is comparable to that observed at the top of the atmosphere.

Reference will be made to the constants of these chambers. They are constructed to give a signal each time they have collected a certain definite charge. Therefore, the time between discharges, t, is related to the ion current collected by $i = k/t$, where k is the constant of the instrument. Strictly, of course, k relates the time for discharge to the ion current collected, but the assumption is made that the current collected is proportional to the ionization in air, and the k is chosen to give ionization in air directly.

B. Summary

This determination of cosmic ray ionization in the atmosphere at balloon altitudes divides into three parts. First,

the ionization in a specific chamber was measured. The chamber was filled with pure argon to a pressure of 1 atm, and was 25 cm in diameter, with an iron wall $\frac{1}{2}$ gm cm^{-2} in thickness. Second, an attempt was made to correct this value for the effect of the iron wall, and for other small effects, and obtain the ionization which would have been produced in an argon filled chamber surrounded only by air. Third, the ionization in argon was referred to air at the reduced pressure existing at balloon altitudes (10 to 100 gm cm^{-2}).

The 1-atm chamber mentioned was a telemetering chamber, calibrated to give ionization in ions cm^{-3} sec^{-1} atm^{-1}. This was done by comparing it to a special reference chamber with an identical wall in which the current could be measured in absolute units and the collecting potential could be varied. The ionization was produced by gamma rays from Th C". The current collected in the reference chamber was measured as a function of collecting voltage, and an extrapolation was made to infinite potential. The common assumption was made that all ions formed are collected under these conditions. The absolute ionization measurement was made in air, and is somewhat more accurate than 1%. Ionization in air at one atm, and in argon at 1 and 8 atm were compared to an accuracy of 1% with the reference chamber. The calibration was preserved until the flight was made by the standard chambers. The final calibration of the 1-atm flight chamber was good

to 1%.

The 1-atm chamber was flown together with one at normal pressure of 8 atm. This comparison makes it possible to tie in to results obtained with the normal chambers. Also, a check on the understanding of recombination and other errors is possible.

If the cosmic-ray ionization in a small volume of argon with an infinitely thin wall is known, the ionization which would be generated in air at the same position can be calculated on the basis of the relative ionization of charged particles only. By "small volume" is meant one small enough not to perturb the paths of any of the particles passing through it. The number of secondary particles produced or stopped in it must be small compared to the total flux. Therefore, the difference between the ionization measured in the actual chamber, and that which would be measured in a small chamber surrounded by air is desired. This difference will be called the wall effect. Several processes were considered, namely: stopping of slow protons in the wall, production of nuclear shower particles, production of star evaporation particles, and electron showers. Wall effect by particles passing through the chamber without an interaction other than ionization energy loss was neglected.

To determine the relative importance of the different processes, the ionization produced by the nuclear particles, electrons, mu's, and stars was computed for atmospheric

depths in the range 10 gm cm^{-2} to 140 gm cm^{-2}. The Gross transformation was applied to the experimental vertical flux. The chemical composition of the primaries was assumed in accordance with the best data available. Star ionization was also estimated. This was all done for geomagnetic latitude, λ_m, = 56°. The additional ionization observed at $\lambda_m = 88°$ is due to primaries of low enough energies that secondary production by them could be neglected, compared to the total number of secondaries.

Stopping of slow protons by the wall, and the effect of the penetrating products of nuclear interactions were considered together. By noting the change in the nuclear component of the ionization, per gm cm^{-2} atmospheric depth, it was seen that these two processes do not contribute an appreciable wall effect in $\frac{1}{2}$ gm cm^{-2} of iron. The effect of star evaporation particles was estimated by taking into account the variation in production rate compared to energy loss of the star prongs, as the wall Z is varied. The production rate was assumed to vary according to the geometrical cross section of the nuclei, but the reactions themselves were assumed to be similar in all materials.

The electronic component was treated in two parts, the high energy, or shower component, and the low energy tail. An argument similar to that used for stopping protons can be applied to electron showers, and it is seen that the wall does not appreciably affect the ionization by electrons of

high enough energy. For energies less than 10 Mev, Compton electrons become predominant. The wall effect which would be observed if all electrons crossing the chamber below 10 Mev were produced by Compton encounters in the wall was computed. This was done by the same general method used for star evaporation particles. It will be an upper limit because the range of a 10-Mev electron is about ten times the wall thickness, and a complete transition will not actually be observed. More exact calculation is not justified by the accuracy of the electronic energy spectrum.

Recombination was considered and found to be negligible in 1 atm of argon.

The relative ionization in air and argon has been measured with 340-Mev protons, which are more or less representative of the cosmic rays in the atmosphere. However, it can be expected to vary somewhat with the velocity of the ionizing particle, according to energy loss theory. Corrections were applied to take care of velocity differences on the basis of energy spectra for the different particles in the atmosphere.

II. THE CALIBRATION

A. Apparatus

Apparatus was constructed to determine ionization which could measure the ion current collected in absolute units. A chamber was provided that had provision for leading the current outside for measurement, and which could be removed for filling and replaced in the same position. The leak rate of a known condenser was used to measure the current, and a string electrometer gave the voltage of the collecting electrode.

The arrangement of the parts is shown in Fig. 1, which is a section through the axis of the chamber. The electrical connections are shown schematically in Fig. 2. The chamber itself is a shell identical to those used with a self-contained electroscope as standards and for flight instruments. An insulator assembly closed the narrow neck of the spherical shell, and could be removed and installed in different spheres if desired. Two of these were made, both incorporating guard rings, one with a teflon insulator, and the other entirely of glass and metal so it could be baked out at high temperature. The teflon was far superior electrically, having no measurable leakage at the voltages used. The glass one was made because a check was desired to ensure the plastic was not causing difficulty by contaminating

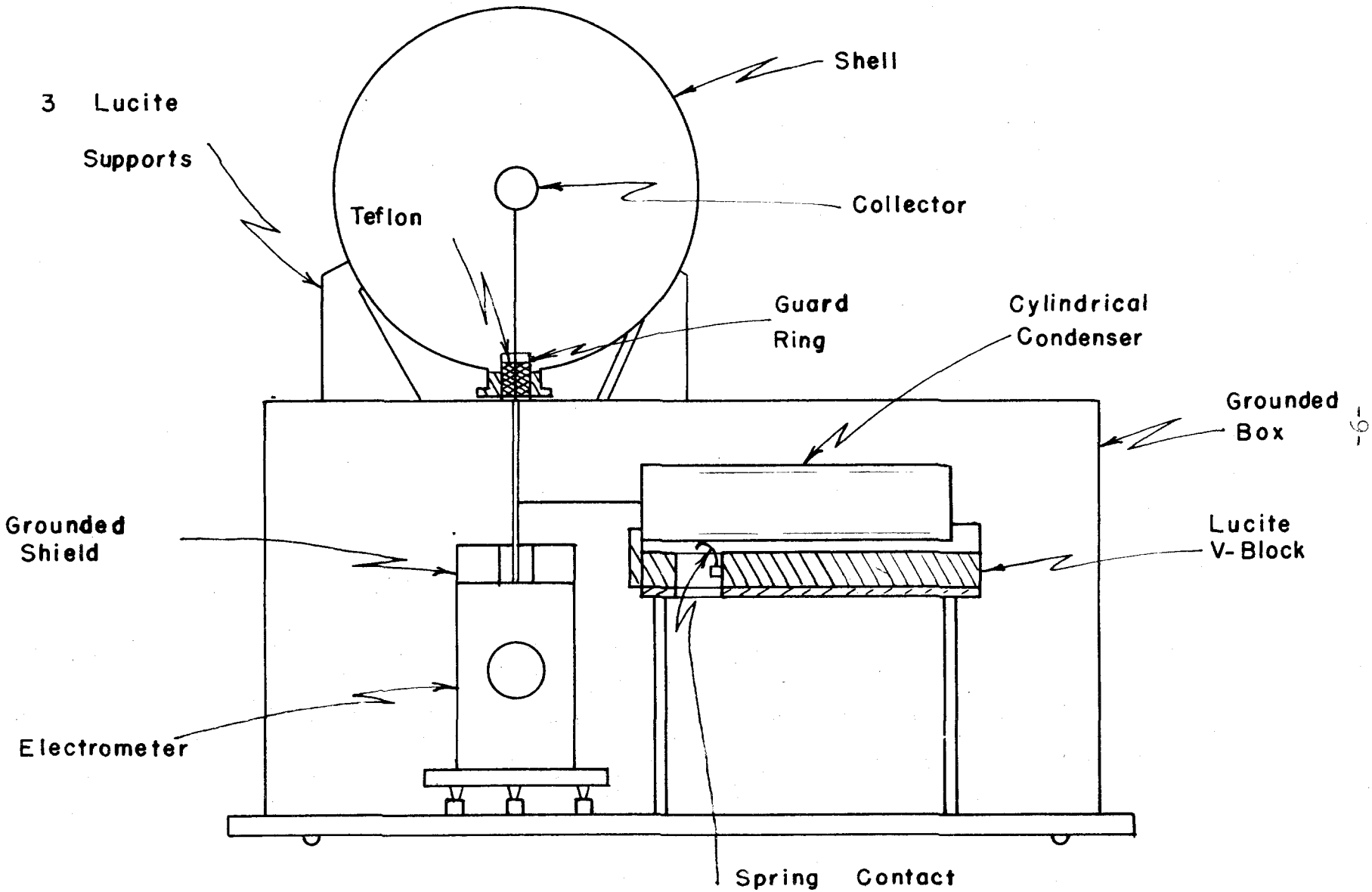

Fig. 1 A section through the apparatus.

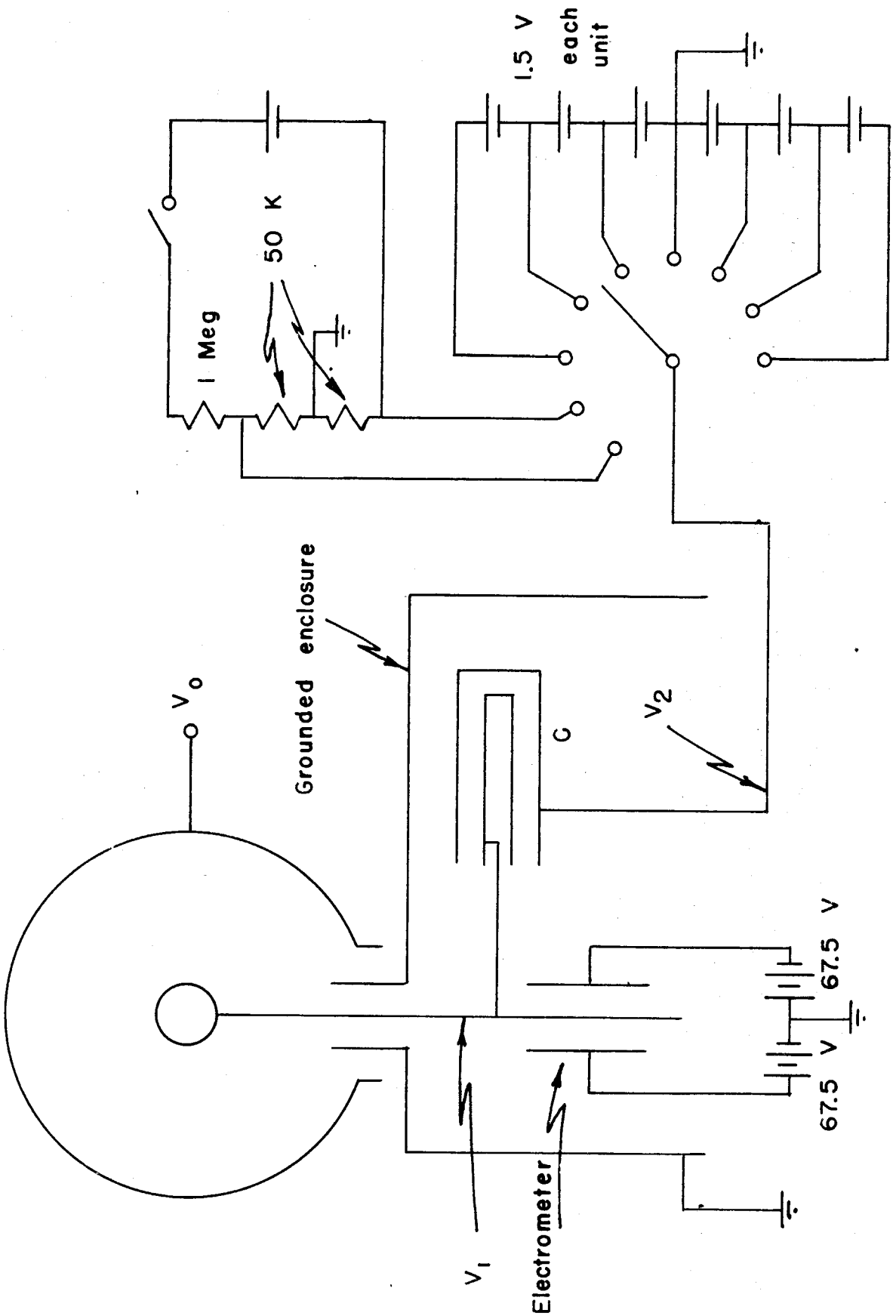

Fig. 2 A schematic diagram of the electrical connections of the apparatus.

the argon. It was used briefly, and discarded when no difference in results was noticed. Leakage across the glass was less than 1% of the ion current, and, as will be seen, cancels out in an actual run. A source of gamma radiation was suspended above the chamber at a distance of about one meter.

A null method was adopted for reading the current, to avoid errors from leakage. A known voltage, V_2, was applied to the condenser in a way to keep the potential of the collector, V_1, near ground. In practice, V_2 was changed in steps by a multipole switch. A plot of the potentials V_1 and V_2 as a function of time in a typical timing interval is presented in Fig. 3. One, three, or $\frac{1}{2}$ of this interval was commonly used, depending on the magnitude of the current being measured. V_2 was switched symmetrically about the ground potential in each case. It can be seen that $\int_{T_o}^{T_1} V_1 dt = 0$ and $\int_{T_o}^{T_1} (V_1 - V_2) dt = 0$, ensuring that all leakage to the collecting electrode will cancel out. The time $T_1 - T_o$ is the quantity actually measured, and the current is derived from it in the following manner:

$$Q = C_{11} V_1 + C_{12} V_2 \qquad (1)$$

$$\Delta Q = C_{11} \Delta V_1 + C_{12} \Delta V_2 \qquad (2)$$

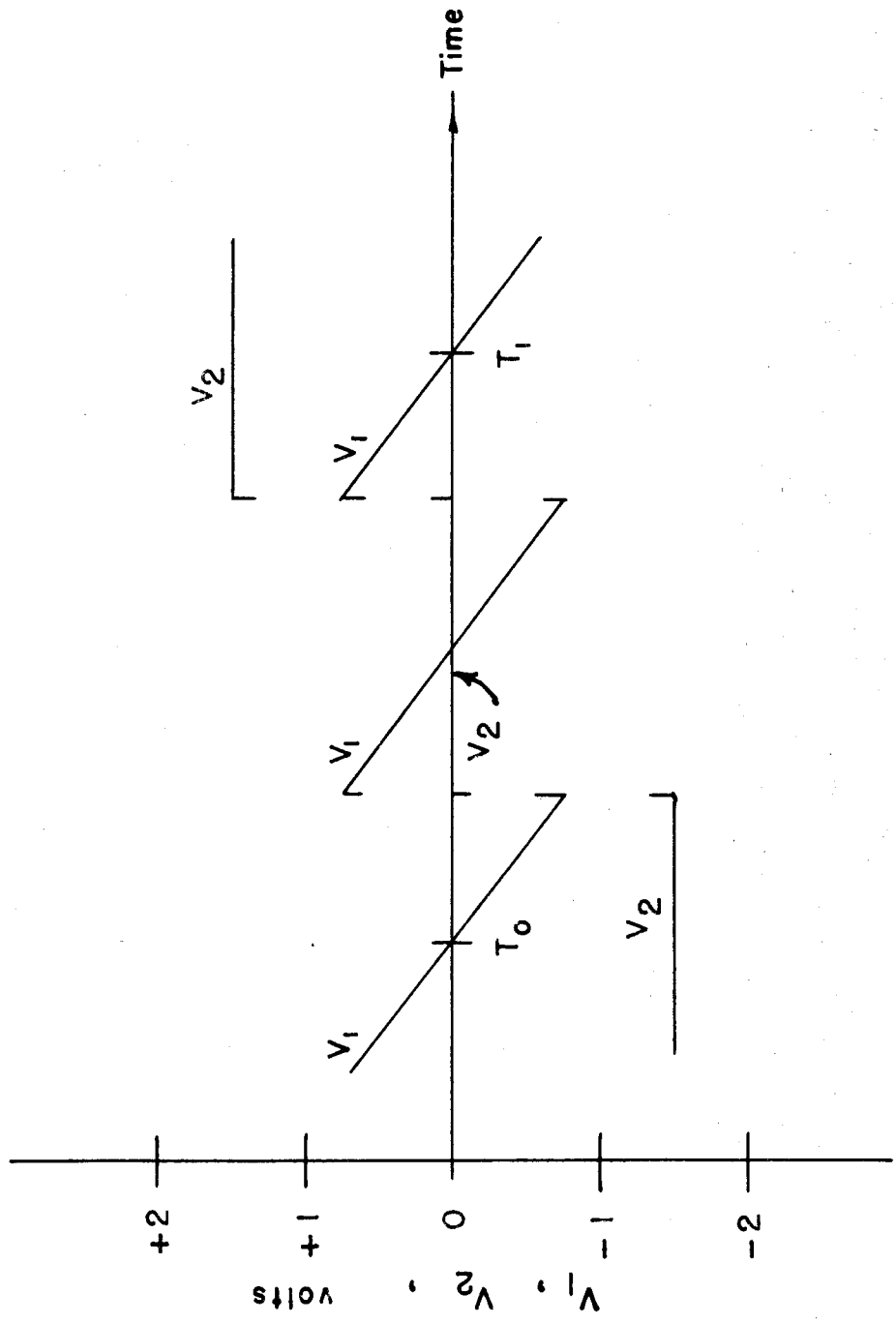

Fig. 3 A plot of V_1, and V_2 (see Fig. 2) vs time in a typical timing interval.

The voltages which enter are those existing at the beginning and end of the timing period, when $V_1 = 0$, because this is the signal for starting and stopping the watch. C_{12} will be called C hereafter. Therefore

$$i = \frac{\Delta Q}{\Delta T} = \frac{C \Delta V_2}{T_1 - T_0} \qquad (3)$$

ΔT was measured to 0.1 sec, and was kept longer than 10 sec at all times, so that the timing error in an average of several intervals was small. V_2 was obtained from dry cells and was known very accurately. The main source of error was in knowing C.

To measure the value of C, two similar cylindrical condensers were made, and the capacity difference between a short one and a longer one was computed from the geometrical formula.

The condensers were made as carefully as possible cylindrical, and with the corresponding diameters equal. They were of brass, and the inner cylinder was supported at each end by three equally spaced 1 mm diameter quartz pins. They were constructed identically, except one was an accurately known amount longer than the other.

Calling the capacity of the small condenser C, and that of the large one C + C'; C' will be calculated from the measured average dimensions.

Diameter of outer conductor, $a = 2.590 \pm .002$ cm

Diameter of inner conductor, $b = 1.868 \pm .002$ cm

Difference in length $l = 14.058 \pm .01$ cm

$$C' = \frac{2\pi\epsilon_0 l}{\ln (a/b)} \tag{4}$$

$$C' = 23.96 \pm 0.09 \quad \mu\mu f$$

The error quoted is derived from the estimated errors in measuring the dimensions. The effects of mis-centering of the conductors and of fringing fields were estimated and found to be negligible in comparison.

To obtain the capacity of the smaller condenser, the ion chamber was used to generate a constant current, i, which was chosen at a convenient value for measuring. The interval ΔT was taken for both condensors, one after the other, using the same set up so that the same ionization was generated, and ΔV_2 was of course the same

$$i = \frac{C\Delta V_2}{\Delta T} = \frac{(C + C')\Delta V_2}{\Delta T'} \tag{5}$$

$$C = C' \frac{\Delta T}{\Delta T' - \Delta T} \tag{6}$$

The values of ΔT, $\Delta T'$, and the value of C computed with the above formula are presented in Table 1. The average

Table 1

Individual Determinations of C.

ΔT, $\Delta T'$ and C are from equation 6

Trial	ΔT sec	$\Delta T'$ sec	C $\mu\mu f.$
1	50.0	163.6	10.54
2	50.4	165.1	10.52
3	50.0	165.3	10.39
4	50.0	165.8	10.34
5	50.4	166.0	10.45
6	50.4	166.3	10.42
7	50.3	166.5	10.37
8	50.4	166.9	10.37
9	39.2	129.5	10.40
		Average	10.42

result was: $C = 10.42 \pm 0.05$ $\mu\mu$f. The error was obtained from the statistical error in the average value, combined with the uncertainty in C'.

B. The ionization determination

The reference chamber was compared to three argon-filled standard chambers, which were in turn used to calibrate the flight chambers. Either the standards or the reference chamber could be placed on the three supporting feet shown in Fig. 1, which supported both at the same distance from the source. The role of the standard chambers can be viewed as follows: A given response of a standard, always about at the same level, implies a certain ionization would be produced in one of the steel shells placed in the same position. The amount of ionization implied was given by the reference chamber, in which it could be directly measured. Therefore, all that is required of the standards is that they respond proportionately to the ionization, reliably, over a limited range.

A small correction to the discharge time of the standards was necessary because they had to be placed on the tripod support in Fig. 1 horizontally, and their normal operating position is vertical. The uniformity of the shells and the distance to the source were such that no correction needed to be made to the ionization itself, but the quartz electroscopes used in the standards are somewhat

sensitive to orientation. The probable reason is that the tiny quartz fiber droops slightly under the pull of gravity.

The actual ionization measurement was made using the following procedure. The reference chamber was filled with air, after evacuating it to be sure no other gas remained. It was then allowed to stand open to the air for approximately one hour to allow it to come to thermal equilibrium, and then sealed off. At the time it was sealed off, the temperature of the shell and the barometric pressure were taken.

Voltage saturation was used as the indication that all ions were being collected from the air. Saturation curves were taken with collection voltages from low values up to 1200 v. A typical curve is shown in Fig. 4. $1/V_o$ is plotted against current collected in the same figure, and a reasonable extension can be made back to $1/V_o = 0$. This intercept was assumed to represent collection of all the ions. In the actual comparisons, a collecting potential of 600 v was used, and it is seen that only a very small correction need be made to find the current at very high voltage.

The results of the comparison are given in terms of the value of k in $I = k/t_{std}$, where t_{std} is the time between discharges for a standard chamber. By the reference chamber,

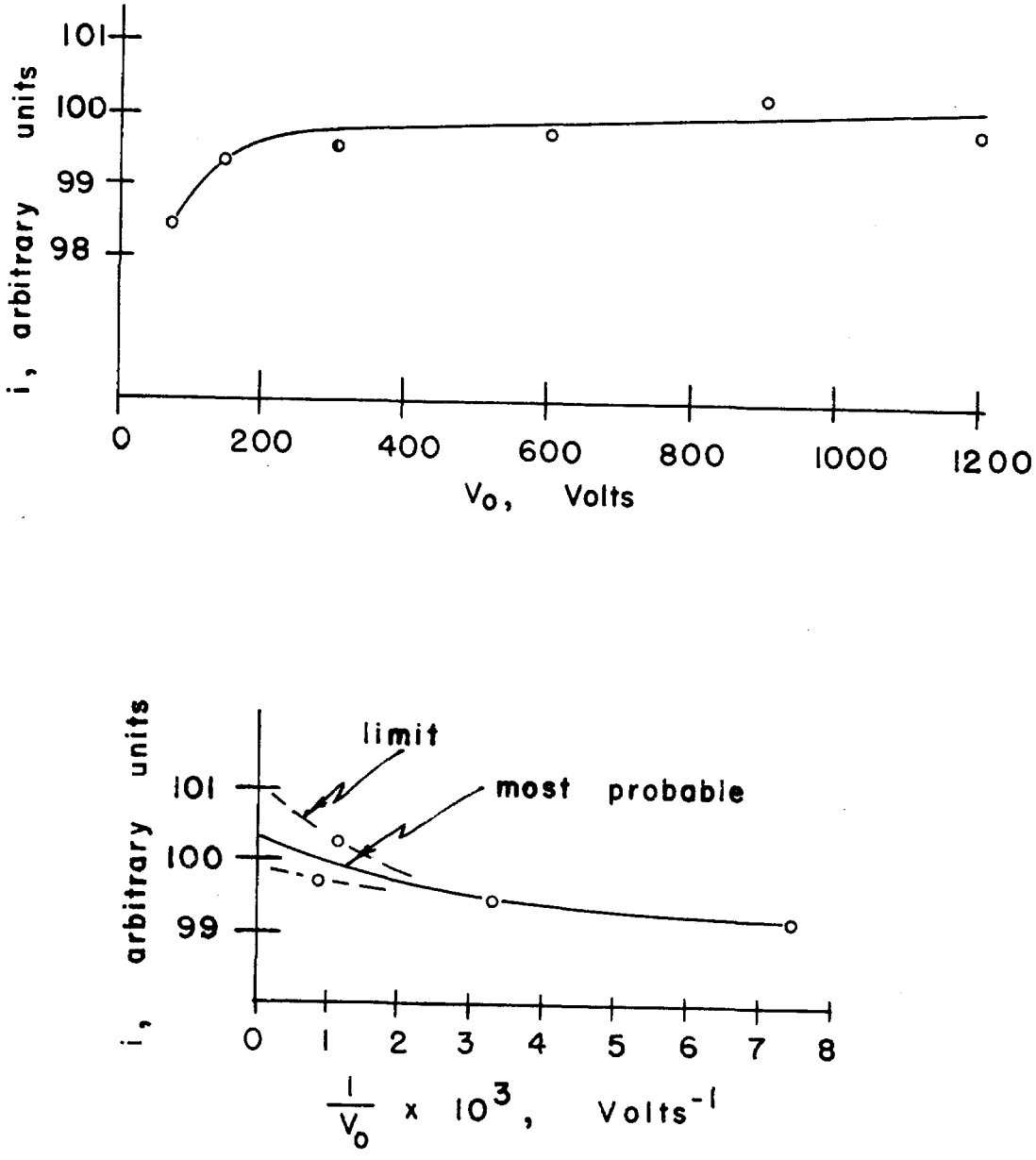

Fig. 4 The current collected, i, vs the collecting voltage, V_o, in the reference chamber. i is also plotted against $1/V_o$, to enable an extrapolation to be made to infinite collecting voltage.

$$I'_{air} = \frac{C\,\Delta V_2}{\Delta T} \quad \frac{1}{e\ Vol\ \rho/\rho_o} \tag{7}$$

I'_{air} is the ionization in air in the steel chamber produced by a gamma-ray source. The unit of I'_{air} is ions cm^{-3} sec^{-1} atm^{-1} at 20°C. $C\frac{\Delta V_2}{\Delta T}$ is the current collected, from equation 3; e is the charge on the electron; Vol the volume of the chamber; and ρ/ρ_o is a factor used to correct the result to 20°C, 76 cm. By the standard chamber,

$$I'_{air} = \frac{k'_{air}}{t_{std}} \tag{8}$$

Therefore,

$$k'_{air} = \frac{C}{e\ Vol} \quad \frac{\Delta V_2}{\rho/\rho_o} \quad \frac{t_{std}}{\Delta T} \tag{9}$$

The volume of the reference chamber, Vol, was obtained by measurements made to the outside of the steel sphere. The average outside diameter was 25.76 cm ± 0.05 cm. The wall thickness of 0.05 cm was subtracted before computing the volume. Also, the volume of the center electrode and the volume made ineffective by electrostatic shielding near the neck was subtracted

Total volume inside shell	8846	cm^3
Ineffective volume	32	
Vol	8814 ± 50	cm^3

ΔV_2 was measured several times during the time comparisons were being made, and is noted in the table. It was measured by a portable potentiometer, and is believed to have negligible error.

ρ/ρ_o was obtained from the temperature and barometer at the time the reference chamber was sealed off. An independent filling was made for trial 5 as a check on this element of the operation. The gamma-ray source was Th C" for trials 1, 2, 5: Co^{60} for 3; and Ra for 4. The raw data is presented in Table 2, and the constants k'_{air} computed by equation 9 are also shown. The value of e used was 1.602×10^{-19} coulombs.

Two runs of ionization (not per atm) vs pressure of air were made with only background ionization. The intercept of these curves at P = 0 is the ionization caused by natural alpha particles from the walls. About ½% of the total ionization came from the walls. It happened that the correction for saturation and this one just cancel.

The average values of k'_{air} for the three standards is shown below, along with k_o, which is the constant which has been used in the existing calibration.

Std	k'_{air}	k_o
111	11460 ± 21	10956
105	11630 ± 50	11250
77	15430 ± 41	14755

Table 2

The Data Used in equation 9, and the Values of k'_{air} Resulting from them

Trial	Inst. No.	ΔT	t_{std}	Corr to std	t_{std} Corr	ρ/ρ_o	ΔV_2	k'_{air}
		sec	sec	sec	sec		volts	
1	111	49.9	24.96	-0.61	24.35	0.9620	3.049	11414
	105	50.7	24.80	0.12	24.92	0.9620	3.049	11496
	77	50.3	31.88	0.91	32.79	0.9620	3.049	15247
2	111	50.3	25.02	-0.61	24.41	0.9620	3.060	11391
	105	50.6	24.90	0.12	25.02	0.9620	3.060	11606
	77	50.6	32.05	0.93	32.98	0.9620	3.060	15300
3	111	63.4	32.02	-0.79	31.23	0.9620	3.062	11570
	105	62.8	31.62	0.16	31.78	0.9620	3.062	11887
	77	63.5	40.77	1.18	41.95	0.9620	3.062	15518
4	111	40.1	20.00	-0.49	19.51	0.9620	3.059	11428
	105	40.9	19.78	0.10	19.88	0.9620	3.059	11417
	77	39.8	25.45	0.74	26.19	0.9620	3.059	15457
5	111	51.8	26.54	-0.65	25.89	0.9739	3.042	11520
	105	51.9	26.20	0.13	26.33	0.9739	3.051	11729
	77	51.5	33.72	0.97	34.69	0.9739	3.060	15619

The simplest way to express this information is in terms of the existing calibration, as only one number is sufficient. The average $k'_{air}/k_o = 1.045$, with an error of about $\frac{1}{2}\%$.

Relative measurements were then made to determine the ionization in argon at 1 and 8 atm implied by a given rate of discharge of the standard chambers. A number of runs of ionization (per atm) vs pressure were a made with the iron shells. The curves are shown in Fig. 5. The ionization scale is arbitrary, and the curves have been normalized at 1 atm. Background radiation has been subtracted out. A correction has been made which was at most of the order of 1% to refer all data to the same value of E/P to get nearly a constant collection efficiency. Run 1c was made with a chamber which was baked out at 300°C for 24 hours while evacuated, before filling with argon. A hot calcium purifier was in operation throughout the run. No significant difference in the results occurred.

After each run, the argon was completely removed, and replaced with air to 1 atm pressure. After equilibrium was established, the ionization in the air-filled chamber was taken. The ratio, which will be called I'_{air}/I'_A (γ), was found to be 0.655 within 1%. Complete saturation was looked for in the argon in the same way it was in air (Fig. 4).

The drop in ionization at 8 atm pressure compared to

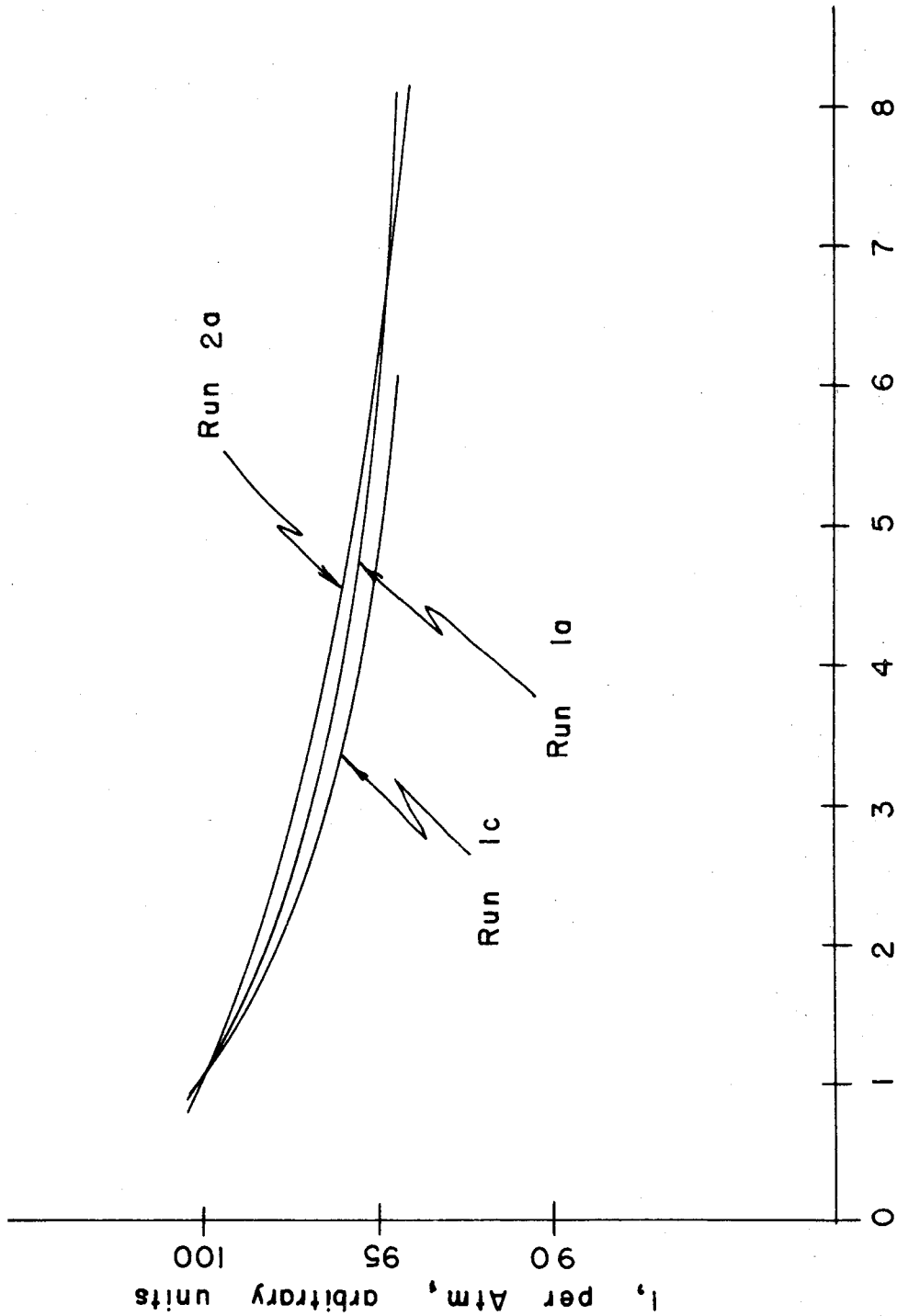

Fig. 5 Ionization, I, per atmosphere, vs pressure. Argon gas was used in an iron shell. Run 1c was made with a calcium furnace purifier, and with a chamber which had been baked out.

1 atm was taken from the curves in Fig. 5, averaged, and found to be 6%, again within about 1%. Some comments on the accuracy of the pressure measurement will be made later.

Using this information, the ionization occurring in chambers at 1 and 8 atm argon can be given. Again the existing calibration will be used as the base. In the Table below, I_o means the ionization which would be obtained using the existing constants, k_o.

Air, 20°C, 1 atm	$\frac{I'_{air}}{I_o}$	$= 1.045 \pm 0.005$
Argon, 20°C, 1 atm	$\frac{I'_A}{I_o}$	$= 1.597 \pm 0.015$
Argon, 20°C, 8 atm	$\frac{I''_A}{I_o}$	$= 1.505 \pm 0.02$

If ionization in argon from very slow or heavy particles were being measured, recombination would have to be considered (Chapter IV).

C. The gamma-ray wall effect.

Several experiments were tried to see if the cause of the dependence of gamma-ray ionization on pressure could be located. Runs of ionization (per atm) versus pressure were made in argon, using different wall materials; namely, iron, plastic, and solder. The iron wall used, of course, was the bare shell mentioned in the description of the instrument. It was 10" in diameter and $\frac{1}{2}$ gm cm^{-2} thick. A wall of plastic with an effective Z near 6 or 7 was made by coating the inside

of one of the steel shells with a layer of Epoxy chemical setting resin. The layer averaged 2-3 mm thick, or 0.3 gm cm^{-2}. A third wall was made by coating the inside of another steel shell with 1 mm, or 1 gm cm^{-2}, of 60% Pb, 40% Sn solder. The effective Z was near 70. These layers were thick enough so the presence of the iron shell on the outside had little effect on the ionization except by a slight attentuation of the gamma ray intensity.

The pressure of the gas was measured by commercial pressure gages. A 0-160 psi gage was used for the higher pressures. It was calibrated first against an absolute gage consisting of a small bore glass tube containing a pellet of mercury. One end of the tube was sealed shut, and the pressure to be measured was applied at the other. Variations in the diameter of the tube were looked for by moving the pellet along the bore, and measuring its length by a traveling microscope. The bore was about 1 mm dia. and the pellet 1 cm long. The perfect gas laws were used to give the pressure after it was found that Van der Waals' equation did not give a significantly different pressure.

An independent calibration was made later using a commercial precision gage and the resulting points were within 1%, in the upper half of the range.

For the lower pressures, a 30"-0-15 psi gage was used, and was calibrated with a mercury manometer on several occasions. The calibration remained constant within about

1% of one atmosphere. The two important pressures were 1 atm and 8 atm, and these could be determined easily to 1%. Actually the pressure gages measure differences from the prevailing atmospheric pressure, so a correction was made to take care of fluctuations in barometric pressure.

The data are presented for the three different walls in Fig. 6. The ionization scale is in arbitrary units, and is expressed in ions per atm. The separate curves are to be understood as all being obtained with the same flux of gamma rays, in the same volume of gas; only the wall material is changed. However, the vertical positioning of the curves is less accurate than their individual shape. Corrections have been made to take care of the smaller volume of gas in the plastic coated chamber. Natural radio-activity in the walls and surrounding material is eliminated by subtracting out the background rate.

It is not felt that impurity coming from the different walls is the cause of any of the difference in ionization. For the iron wall, baking out, elimination of the organic gaskets, and continuous purification did not cause a significant difference in the pressure dependence. For the other two walls, saturation curves were taken, and were not different than those for pure argon. Also, the actual data were taken with sufficient collecting voltage to ensure saturation.

The data indicate that the wall can certainly exert a large influence on the ionization observed. The effect of

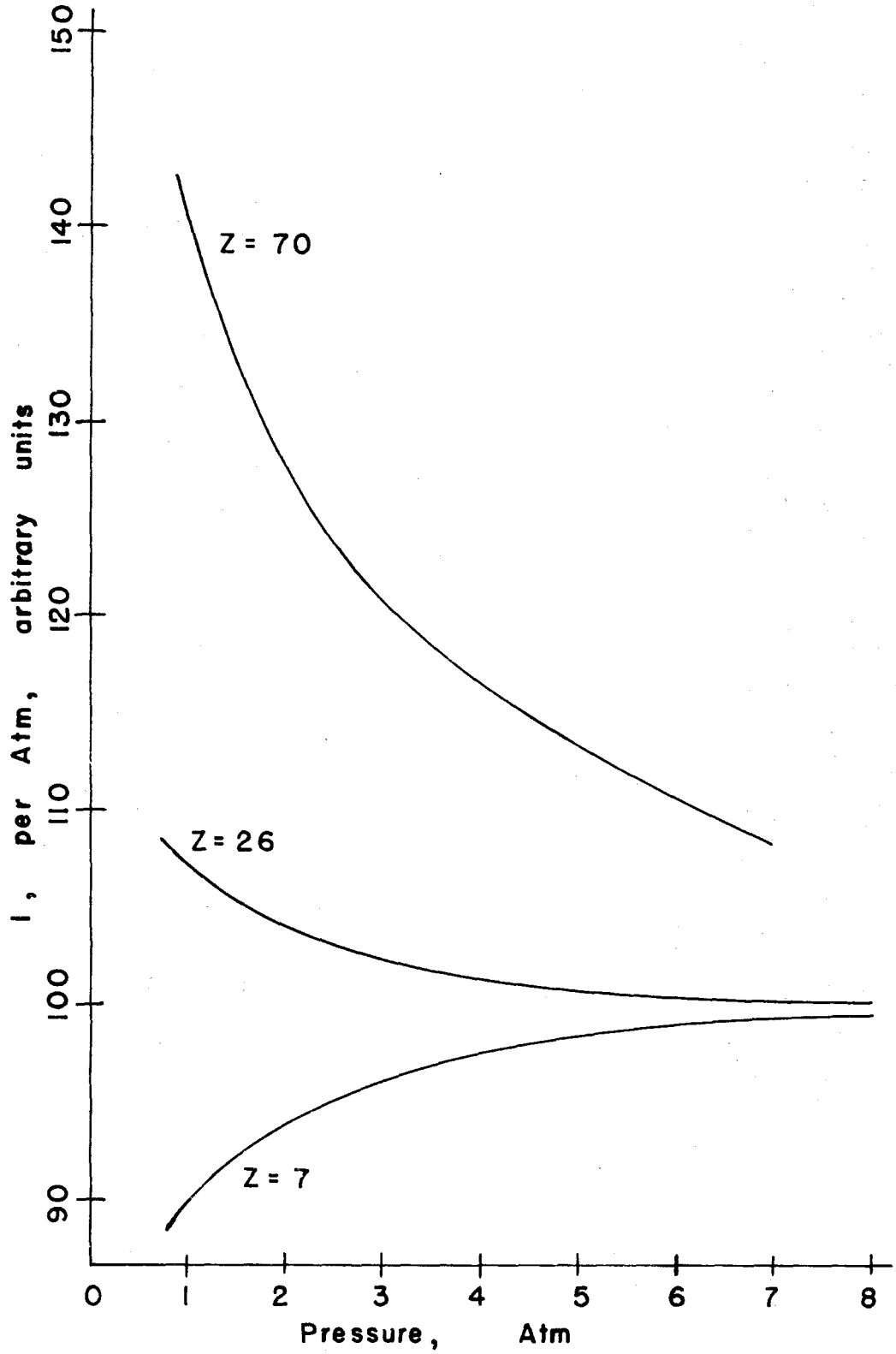

Fig. 6 Ionization, I, per atmosphere, vs pressure, using different wall materials. The average Z of the wall material is noted for each curve. The gas was argon.

the wall shows up as a variation in ionization (per atm) with pressure. At high enough pressure, the ionization would not depend on the wall material, as a negligible fraction would be due to electrons coming from the wall. This was borne out by the data, as the curves of I vs P observed appear to come together at high pressure. At very low pressure, no secondary electrons would be produced in the gas, and the ionization would be entirely due to particles ejected from the wall.

A calculation analogous to the one which will be used in a later section to estimate the cosmic-ray wall effect was made using the gamma-ray spectrum in Fig. 7. The photo-electric cross section was included. The simplified spectrum assumed has the slow rise toward low energy and sharp drop below 150 Kev which a Th C" source filtered by 1 cm lead would have. The results were:

Wall	Z	I, atm^{-1} (relative)
plastic	7	0.9
argon	18	1.0
iron	26	1.1
Sn - Pb	70	1.6

These ionizations would be observed in a chamber at low pressure, when surrounded by the material noted. Being surrounded by argon corresponds to a big volume of the gas, or a chamber at high pressure. So, compared to the ionization,

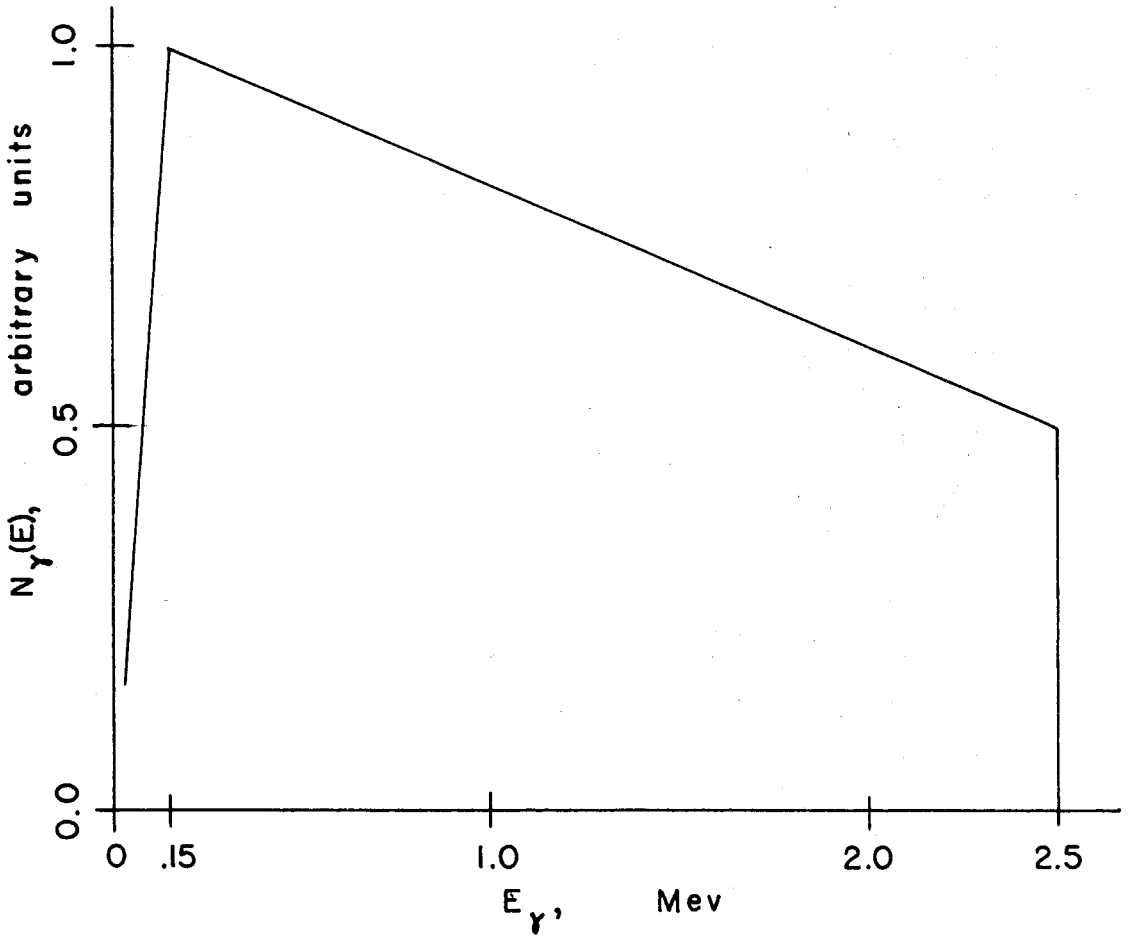

Fig. 7 The gamma-ray spectrum assumed in calculating a wall effect.

I_A, which would be observed at high pressure in argon, one would expect 0.9 I_A, 1.1 I_A, and 1.6 I_A at low pressure with walls of plastic, iron and lead, respectively.

It is seen that considering Compton and photoelectric processes, together with ionization loss of the electrons, can approximately explain the ionization observed at high and low pressure. The relatively large effect of the Z = 70 wall is understandable by noting that the gamma radiation is filtered through 1 cm of lead. The lead cuts off the gamma-ray energy spectrum below a certain energy, E_{min}, because of the sharp rise in photoelectric absorption at low energy. In the Z = 70 wall, further photoelectric absorption occurs, and as a result, large numbers of photo-electrons are ejected from the wall. Further absorption can occur because the cut-off energy, E_{min}, in Z = 70 material, is comparable to the cut-off energy in lead. If the wall were iron, for example, it would not be able to absorb strongly, with the resultant high ionization, because the energy E_{min} would be lower. Photons of low enough energy would have already been removed from the gamma-ray flux by the lead filters.

It has not been shown that all the pressure dependence is due to the wall: only that the observed behavior is of the approximate magnitude to be expected of a wall effect. Other processes are not ruled out.

The possibility of a pressure effect in the ionization process itself was looked for. A 1 cm diameter flat polished

brass surface was mounted on the center electrode of the reference chamber (Fig. 1). A small amount of Po^{210} was rubbed onto the surface from one of the foils on which it comes supplied. The range of the α particles given off was not sufficient to reach the walls. The ionization produced by the α's only was measured as a function of the pressure of the argon gas, and found to decrease 2% in going from 1 to 8 atm. Saturation curves were taken and corrections were made to arrive at the same collection efficiency at all pressures, by using a collection potential proportional to pressure. However, the 2% figure may still be an overestimate. Therefore, it seems very unlikely that the observed pressure effect is to any significant extent the result of an inherent dependence in the ionization process itself on pressure. In other words, w, the energy to form an ion pair is a constant within 2% for pressures of 1-8 atm.

To summarize, the wall is observed to exert a considerable influence on ionization by gamma rays, and the influence shows up as a variation in the ionization observed as the pressure is varied. The variation in energy to make an ion pair is small in comparison. The size of the observed variations is approximately explained by the way that low energy (0 - 2 Mev) photons eject electrons from the wall. The most reasonable conclusion is that mainly a wall effect in gamma-ray ionization is being observed, and this would not be observed in ionization by penetrating particles.

III. THE ANALYSIS OF IONIZATION IN THE ATMOSPHERE

A. Vertical intensities of the components

As primary particles strike the atmosphere, they are absorbed by collision, broken down by fragmentation, and are stopped by ionization loss. Secondaries are produced in interactions, giving rise to electrons and mesons. It is necessary to know the fraction of the total ionization produced by each component which will be considered later in estimating corrections to be applied to the total ionization. The ionization due to stars, electrons, and heavy primaries is particularly desired.

To facilitate the analysis, the particles present in the atmosphere were divided into several groups:

p - Protons and unstable $Z = 1$ penetrating particles

α - $Z = 2$

L - $3 \leq Z \leq 5$

M - $6 \leq Z \leq 9$

H - $Z \geq 10$

e - Electrons

μ - Mu mesons

star - The low energy prongs of nuclear stars

A somewhat idealized picture of a nuclear reaction was used (11). The products were divided into two types; high energy, or shower particles, and low energy, or star particles.

Shower particles are ejected immediately, as a result of nucleon-nucleon collisions. They come out with relativistic energies, approximately in the forward direction. A very highly excited nucleus is left, and subsequently it disintegrates, resulting in a nuclear star. The star prongs are mostly protons and alpha particles in the 10 - 20 Mev range. These will be referred to as the star particles, or star evaporation particles.

The shower particles were assumed to come out exactly in the direction of the primary particle, without angular spread. The same assumption applies to the products of meson decay, and is needed in order to apply the Gross transformation. The evaporation particles were assumed to be somewhat over half protons, the rest α's. They were assumed to be distributed isotropically in space.

A charge spectrum was assumed for the primaries in accordance with the best information available (12-15). The percentage distribution was taken as:

p	=	89.3 %		
α	=	10.0		
L	=	0.23)		(2
M	=	0.35)	Total 0.7% in the ratio	(3
H	=	0.12)		(1

The vertical intensity of the heavy particles was computed using the same diffusion equations which have been used

by others to interpret plate data. Since fragmentation can only reduce the charge, and since multiply charged fast secondaries are very rare for light incident particles, the L, M. H group can be treated independently of the others. The notation used is that of Noon and Kaplon (16).

$$\frac{dN_i(x)}{dx} = -\frac{N_i(x)}{\lambda_i} + \sum_{i' \geq i} \frac{N_{i'}(x)\, P_{i'i}}{\lambda_{i'}} \qquad (10)$$

$N_i(x)$ - The vertical flux at depth x gm cm^{-2} of particles of type i

λ_i - The interaction (collision) length of particles of type i.

$P_{i'i}$ - The probability that in a collision a particle of type i' produces a secondary of type i.

The solutions to these equations are given by Noon and Kaplon. The constants λ_i are obtained from plate data, and agree closely with the geometrical cross sections. $P_{i'i}$ has been obtained by statistical analysis of the products of a large number of interactions observed in emulsions.

The resulting intensity of L, M. H particles is plotted in Fig. 8 in terms of the flux of the same particle at the top of the atmosphere. Fragmentation is important only for N_L, which is one of the reasons its intensity at the top of the atmosphere is so difficult to estimate. However, the

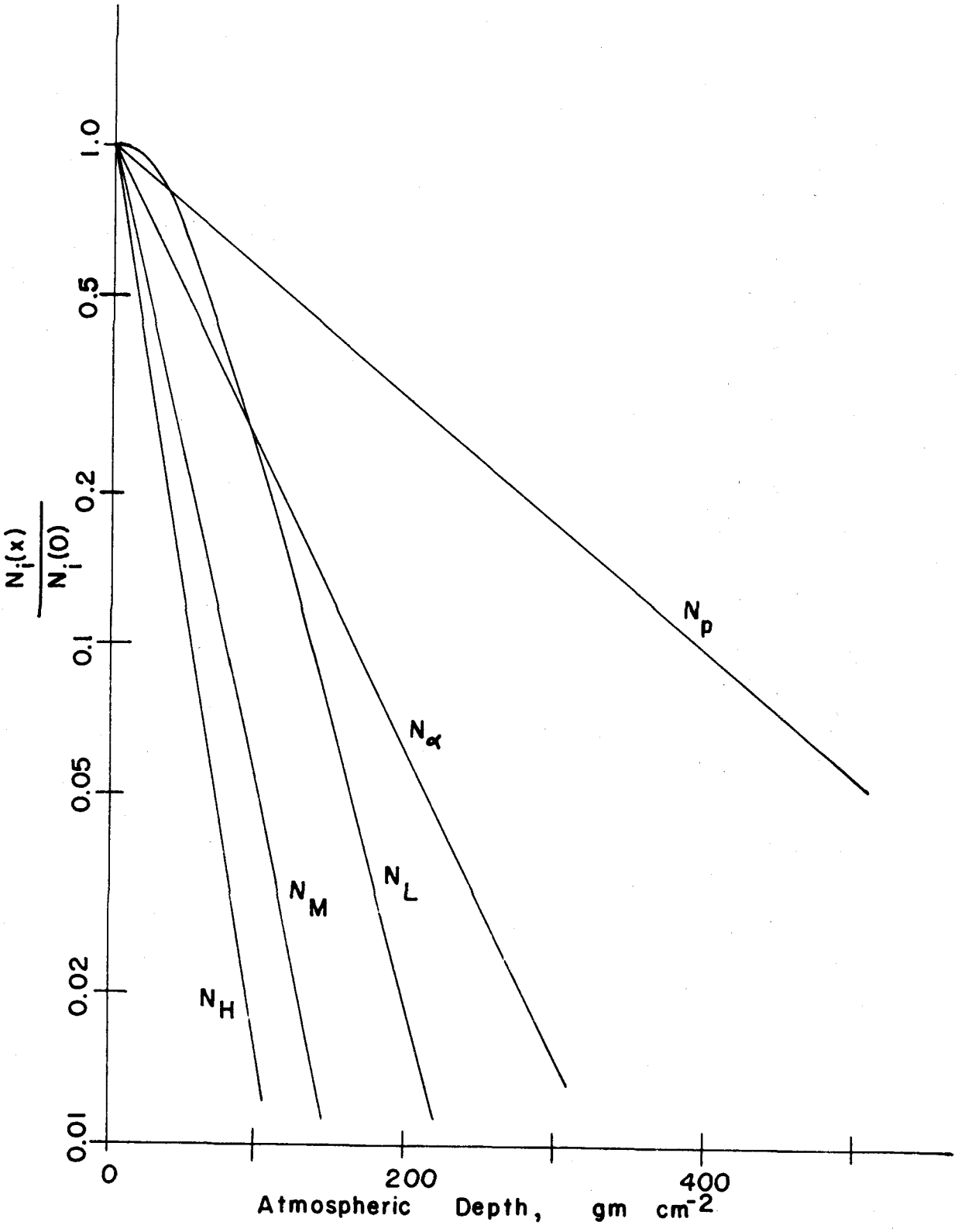

Fig. 8 The vertical intensity of the primary components vs atmospheric depth. The intensity of each component is given in terms of its intensity at the top of the atmosphere.

contribution of the L group to the ionization is so small that inaccuracies in its intensity are unimportant.

N_H is described by an attenuation length of 24 gm cm^{-2}. This compares to 21 $\pm$ 2 gm cm^{-2} for the same quantity measured by Frier et al. (17). We will use 24. N_M will be taken proportional to $e^{-\frac{x}{34}}$. This does not differ from the actual solution of the diffusion equation more than 0.01 $N_M(0)$.

The alpha-particle intensity was obtained independently. Davis, et al. (18) give an attentuation length of 50 gm cm^{-2}, which is reasonable when compared to an interaction length of 44 gm cm^{-2}, by Peters (19). In the absence of further information, we will say that the intensity varies as $e^{-\frac{x}{50}}$. It is legitimate to extend this intensity to the top of the atmosphere because fast secondary α's are rare (20).

Proton and μ intensities are divided into fast and slow p and μ according to whether their range is more or less than 90 gm cm^{-2} of lead, but the slow proton flux is cut off at energies below about 100 Mev. These intensities, as well as the electronic, are given by Komori (7). His fast proton intensity is represented closely by an attentuation length of 120 gm cm^{-2}, which agrees with the altitude variation of stars produced by protons, at this latitude (21). Komori uses the rate of burst production to arrive at his curve. Extrapolation of proton intensity to zero depth is not possible, because of the secondaries produced as soon as material is encountered. For computation purposes, it will be extended

to zero depth by continuing the $e^{-\frac{x}{120}}$ curve. Komori's data are plotted up to 20 gm cm^{-2}, and if they are correct this far, little error will be introduced in the ionization calculated for this depth, and somewhat higher. The α and fast proton intensities used are also plotted in Fig. 8, in terms of the assumed flux at the top of the atmosphere.

The vertical intensities of e, μ, slow p, and slow μ are also given by Komori, and were used as is. He gives them only up to 20 gm cm^{-2}, so the above remarks about extending the results upwards apply here, also. Instead of plotting absolute intensities, these are given in terms of the assumed fast proton flux at x = 0, and are shown in Fig. 9.

The Gross transformation was next applied to each of the vertical intensities shown in Figs. 8 and 9, to obtain omni-directional intensities. Use of this transformation involves the assumption that the flux at any point in the atmosphere in any direction depends only on the mass traversed in that direction to the point in question. For this to be true, primaries must be distributed isotropically, and the lateral spread of secondaries must be negligible.

The resulting omni-directional fluxes were then weighted by the average specific ionization of the different groups: α = 4, L = 16, M = 49, H = 196. Each component was also weighted by its abundance at x = 0 compared with that of the protonic component. A quantity proportional to ionization was thus obtained. So far, no attempt has been made to find

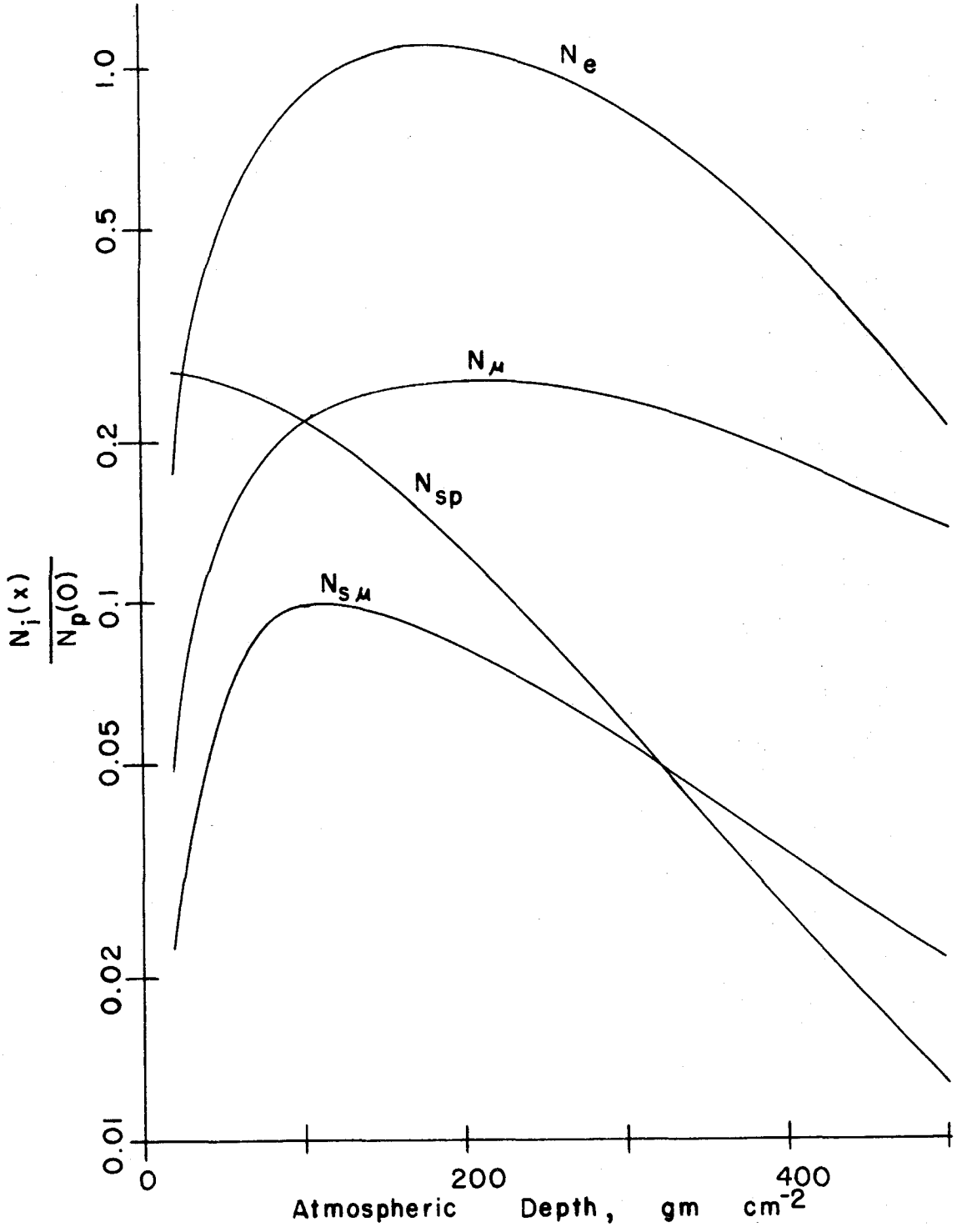

Fig. 9. The vertical intensity of the secondary components, vs atmospheric depth. Intensities are given in terms of the protonic flux at the top of the atmosphere.

absolute ionization; only altitude dependence by components.

B. The star ionization

The star ionization was computed on the basis of work by Lord (21) and Coor (22). Lord measured production rates of stars with two or more black prongs in emulsion at several altitudes. Since the energy going into the evaporation particles is not highly sensitive to the energy of the incident particle, his results are proportional to the energy going into star prongs, as a function of altitude. Two methods are available to find the average energy, but the results of Coor would seem to give the most reliable estimate.

He has measured burst size distribution as a function of altitude in a pulse ion chamber. It had dimensions almost the same as the ones used here, and was filled to 1.5 atm pressure with argon. He concluded that electron showers contribute a negligible number of bursts, and that those observed are due to heavily ionizing particles. His absolute burst frequency is in agreement with star production rates in emulsion. He concludes that all his bursts are due to stars, except at very high altitudes ($\sim$15 gm cm^{-2} depth), where a significant fraction is due to heavy primaries. Our calculation of the attentuation of primary heavy particles agrees with this conclusion, since no $Z \geq 3$ particles exist at 100 gm cm^{-2}.

Coor has integrated his burst size spectrum to find the total ionization due to bursts leaving more than $\frac{1}{2}$ Mev in the chamber (about 6 diametral traversals of a minimum singly ionizing particle). The result was 25 ions cm^{-3} sec^{-1} atm^{-1} of air at 100 gm cm^{-2} depth. This is identical to the star ionization, by the above arguments, but similar calculation cannot be called the star ionization at higher altitudes, because of the contribution of heavy primaries. Coor's flight was made at geomagnetic latitude, $\lambda_m = 50^\circ$. To apply the result to $\lambda_m = 56^\circ$, it was increased in the same ratio as the total ionization, to 28 ions cm^{-3} sec^{-1} atm^{-1}.

An interesting comparison is available from an estimate of average star energy using emulsion data. Lord gives the distribution of stars by the number of prongs, and the average is 6. The information presented by Rossi (23) on the energy distribution of the prongs indicates that 10-15 Mev is their average energy. This implies that stars release about 75 Mev on the average. Brown et al. (24) have also measured the average energy of the low energy star particles, and arrive at a somewhat higher result. Using the 75 Mev figure, and 32 ev per ion pair, one obtains 25 ions cm^{-3} sec^{-1} atm^{-1} at 100 gm cm^{-2} depth. This will equal the actual ionization in the air only if the energy per star is the same in air as in heavier elements. In view of the uncertainties, the good agreement is fortuitous.

The altitude dependence found by Lord was normalized to

28 ions cm^{-3} sec^{-1} atm^{-1} at 100 gm cm^{-2}, and the resulting curve appears in Table 3 as the star ionization.

C. Results

These results apply to a geomagnetic latitude, $\lambda_m = 56^\circ$. A typical ionization record from Bismarck, N.D., $\lambda_m = 56^\circ$, is shown in Fig. 10. The computed total ionization is shown on the same graph. The absolute values for particle ionization have been obtained by requiring the total of particle and star ionization to equal the experimental curve at 100 gm cm^{-2} depth. The fit at the highest altitudes is quite sensitive to the percentage of L, M, H particles assumed in the primary radiation. The results which would have been observed with 1.0% instead of 0.7% of such particles as also shown. 0.7% gives the best fit, and is not in disagreement with independent measurements of this quantity. However, it should be pointed out that an error in the form of the proton intensity will be reflected in a change in the percentage of L, M, H for best fit.

These results are to be applied to $\lambda_m = 88^\circ$, at a time when about 20% more ionization was being observed (at 10 gm cm^{-2}) at the higher latitude. The geomagnetic cutoff at $\lambda_m = 56^\circ$ for protons at the vertical is 0.8 Bev. Most of the particles getting in at higher latitude have considerably less energy than this, and are absorbed rapidly in the atmosphere. The assumption will be made that all these particles are absorbed without producing additional secondaries. This of course, is not really true, because a 350-Mev

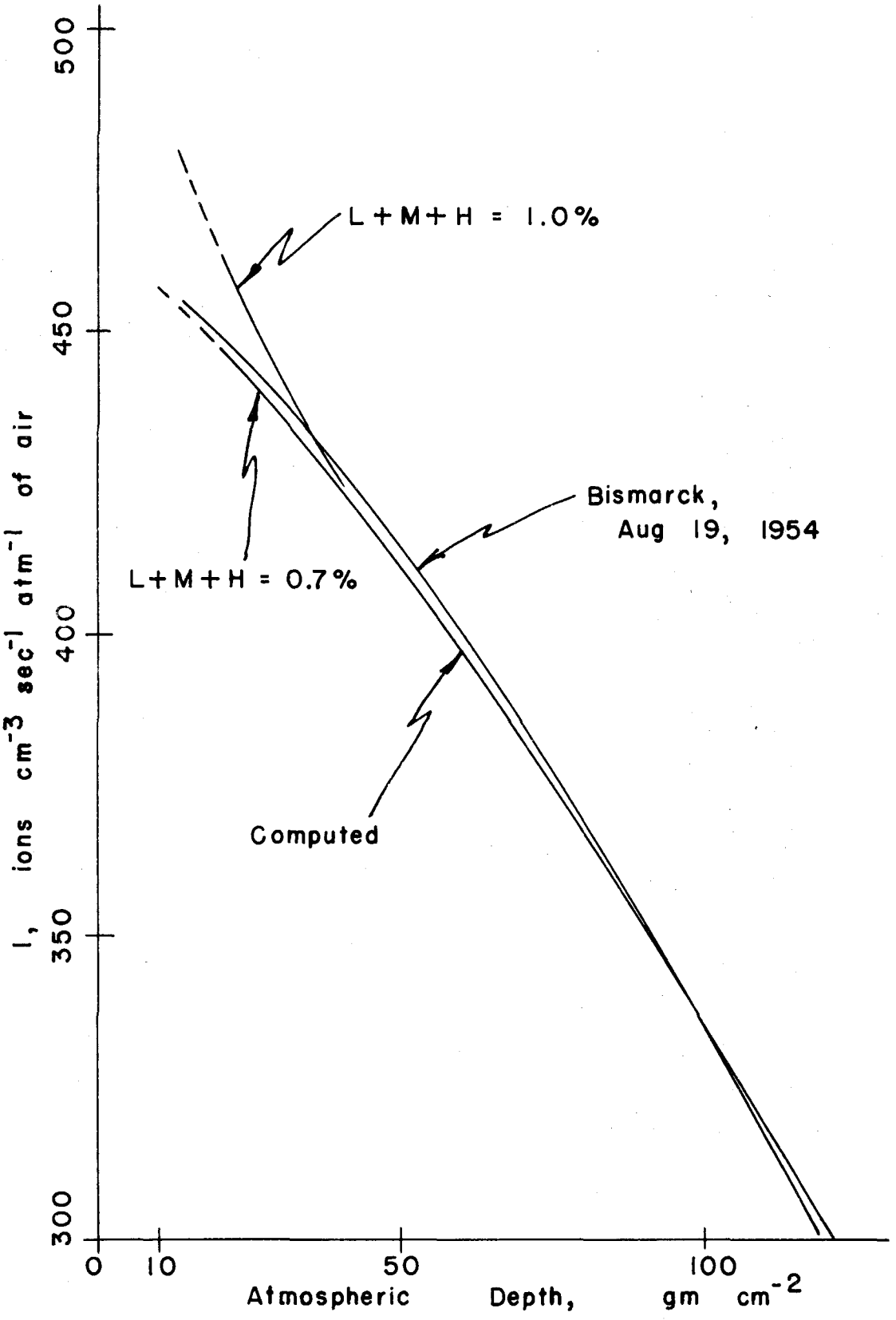

Fig. 10 The computed total ionization compared to the measured ionization at Bismarck. The effect of changing the heavy particle flux is illustrated.

proton has an ionization range equal to its collision length. The error in the secondary ionization cannot be as much as half the total ionization added, which is quite accurate enough for the purpose at hand.

The ionization by components is tabulated in Table 3. The additional ionization observed at $\lambda_m = 88^\circ$ is listed as such, and strictly speaking, the other data apply to $\lambda_m = 56^\circ$. The same information is plotted again in Fig. 11, in terms of percentage of the total ionization at a given depth. Fig. 11 applies to $\lambda_m = 88^\circ$, with the qualifications noted above.

Table 3

The Ionization Spectrum in the Atmosphere

(The ionization of each component is given in ions cm^{-3} sec^{-1} atm^{-1} of air)

Component	Z	Depth, gm cm^{-2} 10 (extrap)	20	40	60	80	100	140
Protonic	1	195	141	98	73	58	44	29
α	2	61	40	20	11	6	4	-
L	3-5	7	6	3	2	1	-	-
M	6-9	21	12	5	2	-	-	-
H	10	22	11	4	-	-	-	-
electronic	1	56	111	161	179	181	175	152
fast μ	1	15	29	40	46	48	48	44
slow μ slow p	1	46	62	59	52	43	36	25
Stars	1,2 slow	35	35	34	32	30	28	22
difference between $\lambda_m = 88^\circ$ and $\lambda_m = 56^\circ$		45	32	16	6	-	-	-
Total ($\lambda_m = 88^\circ$)		503	479	440	403	367	335	272

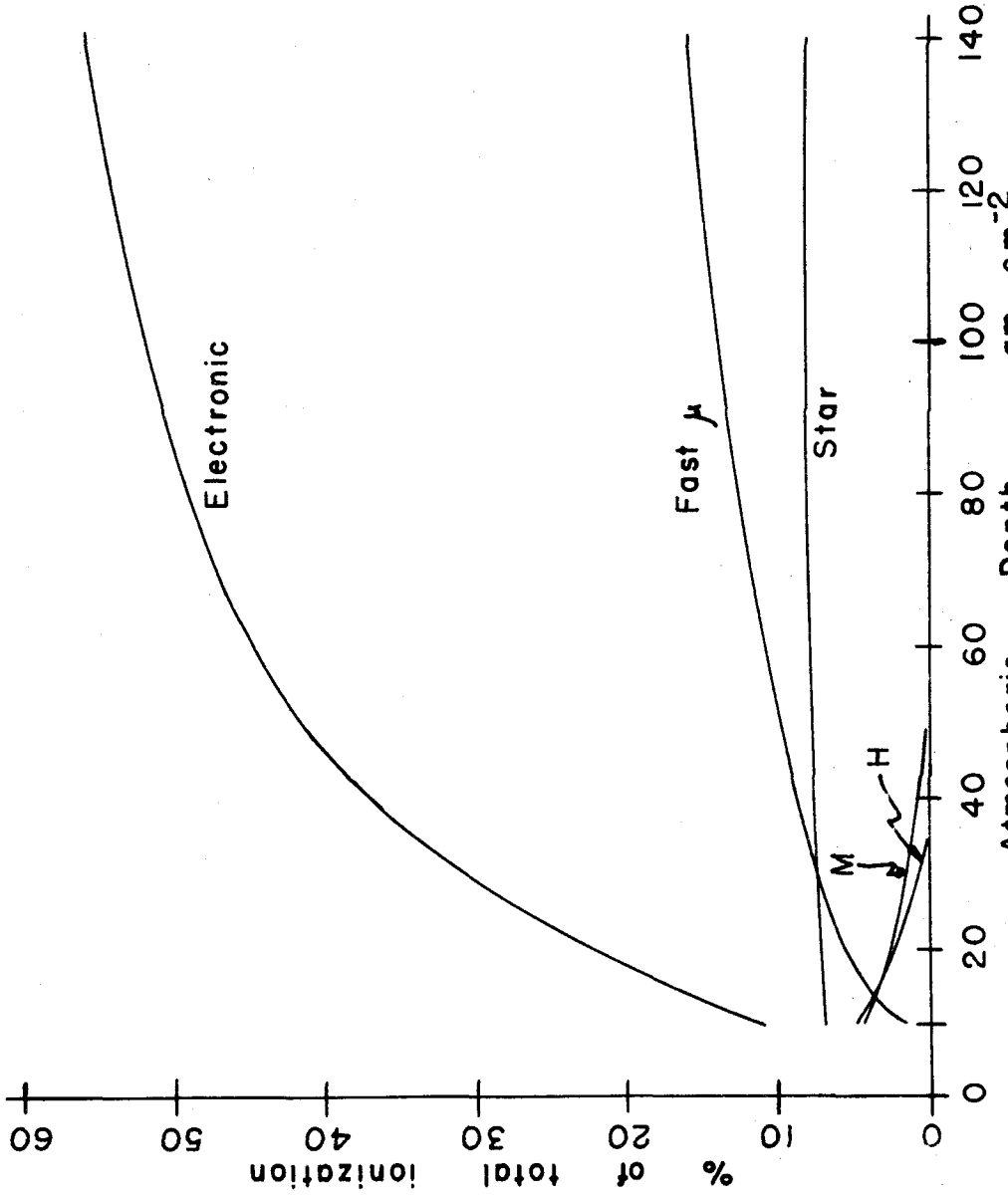

Fig. 11 The fraction of the total ionization, in percent, due to electrons, μ mesons, stars, and the M and H components, as a function of depth.

IV. RECOMBINATION IN THE FLIGHT CHAMBERS

A. Summary of types of recombination

The presence of an unknown recombination loss in cosmic-ray ionization has always placed some doubt on its absolute measurement. Recombination was considered along with diffusion to the walls, and α's from natural decays in the wall. It was found that no correction was needed in the 1-atm chamber for these effects, but that columnar recombination was significant in the 8-atm chamber.

Recombination is generally divided into three types, initial, columnar, and volume. Initial recombination involves positive and negative charges formed from the same atom. The quantity R_i will be defined as the fractional loss of ionization due to initial recombination:

$$R_i = \frac{I-i'}{I} \tag{11}$$

where I = ions formed cm^{-3} sec^{-1} atm^{-1}.

i' = ions collected cm^{-3} sec^{-1} atm^{-1}; assuming that the only loss is due to initial recombination.

We wish to apply the argument to be presented to a specific instrument, and so the field, pressure, impurities in the gas, and the geometry are fixed. Under these conditions R_i is a constant.

Columnar ionization, R_c, occurs because of the high density of ions at formation in the track of a heavy or slow particle. R_c has a meaning similar to R_i. In a specific instrument, this loss would depend only on the specific ionization of the particle, σ ; $R_c = R_c(\sigma)$.

Volume recombination, R_v, occurs when ions from different tracks combine, and is treated as if the ions were formed uniformly throughout a volume. R_v depends on the level of the ionization; $R_v = R_v(I)$.

Diffusion to the walls, D, can be treated at the same time, and the term D will be defined in the same way as the R's. In a given chamber at reasonable levels, it will be constant. There is also a small ionization in any chamber which is produced by natural decays in the wall. This will be represented by W_α. W_α is to be understood as a constant ionization, not a fraction of the total.

Something can be said about the approximate size of the losses that have been mentioned. R_i has been investigated by Bradbury (25), and was found to be strictly zero in pure noble gas. However, the level of impurity which may be important is not known very well. In practice it should certainly be quite small. R_c is the important quantity for the cosmic radiation and will be considered below. It is negligibly small at 1 atm, but may not be so at 8 atm. R_v was looked for by seeing if two gamma-ray sources measured separately are summed correctly if measured at the same time.

This has been done at widely varying levels, and R_v is felt to be 1% or smaller in 8 atm at the usual levels of ionization. D was checked by reversing the polarity of the special test chamber, and found to be on the order of 1%. W_α was found of the order of $\frac{1}{2}$% at 1 atm, by extrapolating the background rate to zero pressure. It is seen that all the losses are small quantities.

The cosmic-ray ionization is determined by first placing the flight chamber at a certain distance from a gamma-ray source, where a known ionization I_{std} is produced by the gamma rays alone. The electroscope is then observed to discharge at an interval, t, which is inversely proportional to the current collected:

$$i = \frac{(\text{const})}{t} \tag{12}$$

$$I_{std} = \frac{(\text{const})}{t}\,(1+R_i+R_c(\sigma_\gamma)+R\,(I_{std})+D)-W_\alpha \tag{13}$$

Similarly, for cosmic rays at high altitudes,

$$I_{cos} = \frac{(\text{const})}{t}\,(1+R_i+R_c(\sigma_{cos})+R\,(I_{cos})+D)-W_\alpha \tag{14}$$

I_{std} is chosen at approximately the same value I_{cos} is expected to be. Since W_α and $R_v(I)$ are not large anyway, a new constant, k, can be defined which includes the constant losses, and to a good approximation, also includes R_v and W_α;

$$I_{cos} \qquad \frac{k}{t_{cos}} \quad (1 + R_c(\sigma_{cos})) \qquad (15)$$

As R_c (σ_{min}) is extremely small, k can be correctly determined directly from the measurements of I_{std} and t; $I_{std} = k/t$.

To summarize, the flight chamber is calibrated by noting its response to a known gamma-ray ionization in a calibration set up. Therefore, a certain discharge rate implies the correct ionization in spite of any constant errors in the instrument. Loss from columnar ionization, which depends on the type of radiation, is the only one that needs to be evaluated.

B. Recombination in cosmic-ray ionization

At 10 gm cm^{-2} depth, a significant fraction of the ionization is caused by primaries of Z = 10 or more. These particles are completely eliminated by absorption at 100 gm cm^{-2}. About 8% of the total is produced by the low-energy evaporation prongs from nuclear stars, at either altitude. Emulsion data (11) indicate that the average star has somewhat over half of its prongs protons, whose average energy is near 10 Mev. The rest are α's of average energy 15 Mev. We will assume that half the star ionization is from 15-Mev α's; half from 10-Mev protons. The average specific ionization of these is 420 i_{min} and 60 i_{min}, respectively, compared to 820 i_{min} for Po α's.

Data were available on the collection of ionization from Po α's in a pulse chamber having spherical geometry, and the source at the wall (27). The experimental form of i/I obtained is shown in Fig. 12. The abscissa is E/P existing at the position of the particle tracks. The chamber was filled with pure argon. Similar data were also taken in the integrating chamber (Fig. 1) at 8 atm, but higher fields (x1.5, even using Jaffe's formula) were required to collect the same fraction of the ions. Quite a high volume density of ionization resulted from the short α-particle range, and the level of ionization used. It was felt that this caused additional recombination, and was the reason for the difference. The saturation curve for the pulse chamber was used, because it gives a lower limit to the recombination.

Jaffe has developed a theory of columnar recombination which fits experiment reasonably well (26), and should form a good basis for estimating recombination from other particles. The form of his result is the following:

$$\frac{i}{I} = \frac{1}{1 + CNf\left(\frac{E}{P}\right)} \qquad (16)$$

where C is a constant; i, I as before. N is the number of ions formed per cm path, E is the collecting field, and P the gas pressure. This applies to a constant field, and is averaged over the angle between track direction and field.

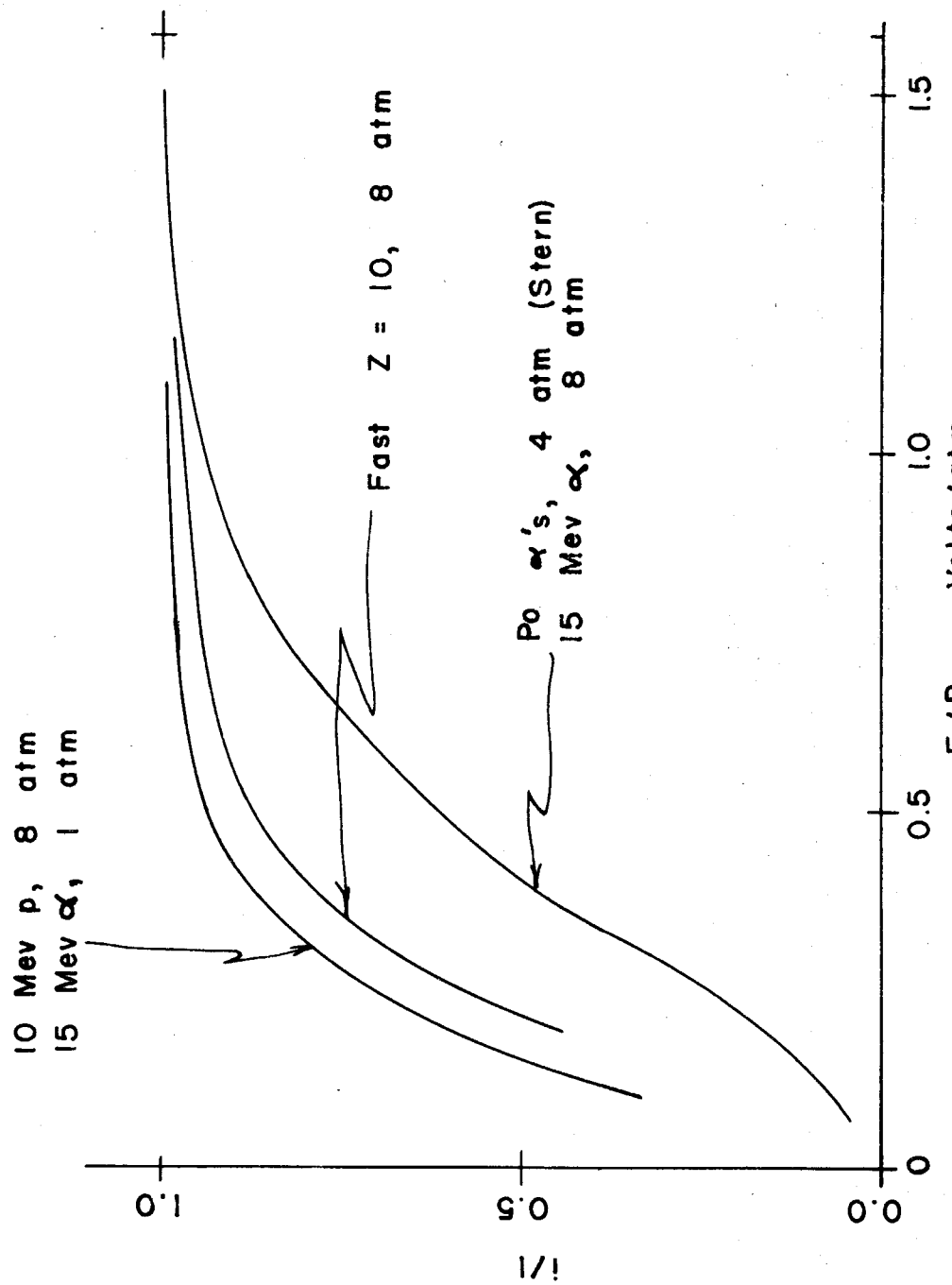

Fig. 12 The ion current collected from dense tracks as a function of collecting field.

Equation 16 was used to find the other curves shown in Fig. 12, starting from the Po α data. Curves were plotted for 10-Mev protons, 15-Mev α's, and fast Z = 10 particles in 8 atm of argon. A curve was also plotted for 15-Mev α's in 1 atm of argon. It happened that two pairs of curves coincided.

The actual flight chambers have a rod 1 mm in diameter; 7 cm long for the central electrode. The field which exists at the outside of these chambers was measured using an electrolytic bath. It was found, as might be expected, to be greater near the neck, from which the rod projects, than directly opposite (4 v/cm vs 1 v/cm). The field halfway between was 1.5 v/cm, with 300 v applied between sphere and collector. For purposes of calculation, the field was assumed to be that of spherical geometry, and equal to 1.5 v/cm at the chamber wall. This gives the correct field averaged over the volume near the wall, and closer to the center, there is no recombination. The amount of loss can now be easily calculated because it depends only on the distance from the center of the chamber.

It is apparent from inspecting Fig. 12 that there is no recombination in the 1-atm chamber, because even tracks as dense as a Po α are completely saturated at the outside of the chamber. Even for fields as small as 0.4 v/cm, only 10% of the ionization of a 15 Mev α would be lost, according to Jaffe's curve. This would result in the loss of a negli-

gible fraction of the total ionization. An extreme variation from the Jaffe expression would be required to make imperfect collection occur. There can be little doubt that there is no recombination difficulty in a chamber filled with argon at 1-atm pressure.

An order of magnitude estimate of the recombination occurring in an 8-atm chamber can be given by integrating numerically;

$$\left\langle \frac{i}{I} \right\rangle_{av} = \frac{1}{V}\int_{Vol} \frac{i}{I}\,dV = \frac{1}{V}\int_{Vol} \frac{4\,r^2 dr}{1 + CNf\,(E/P)} \qquad (17)$$

The result will be an upper limit, as the data are obtained in a pulse chamber. Further, recombination may be quite sensitive to impurity. An example of the numerical results for two specific types of particles is;

$$15 \text{ Mev } \alpha, \left\langle \frac{i}{I} \right\rangle_{av} = 0.41$$

$$10 \text{ Mev } p, \left\langle \frac{i}{I} \right\rangle_{av} = 0.78$$

According to this estimate, the 8-atm chamber is, as a whole, only half saturated for the α-particle ionization from stars, and 3/4 saturated for the protons.

Using this information, and the ionization spectrum in Fig. 11, the recombination loss to be expected at different altitudes can be obtained. The important components are the M and H groups, and of course, stars. At 100 gm cm^{-2}, stars

alone are important, and a loss of 3% of the total results. At 10 gm cm^{-2}, the heavy primaries will cause 2% more loss, according to this estimate.

The conclusion which can be drawn is that recombination may cause a few percent loss, and will be somewhat more serious at the highest altitudes. It will definitely not be all due to heavy primaries and will not disappear as soon as they are absorbed. More will be said of this matter later when the comparison of 1 and 8 atm chambers is discussed.

V. THE WALL EFFECT ESTIMATE

A. Definitions

The ionization measured in a real, physical chamber may be different than that observed in a similar volume of gas not surrounded by the metal wall. In this experiment, it is desired to sample the charged particle flux which is present in the atmosphere, without disturbing it. A small enough volume of gas would do this if it had an infinitely thin wall. The difference between the measured ionization and that which would be observed in such a hypothetical chamber will be called the wall effect.

A small wall-less chamber is specified rather than considering an arbitrarily big volume to eliminate the influence of the wall, because the ionization in argon must later be converted to ionization in air. In a big chamber, interactions of photons and energetic particles in the gas itself would have to be taken into account in the conversion to air. If the range of all secondary particles is long compared to the dimensions of the chamber, they will have been produced mostly in the surrounding air, and only the relative energy loss by ionization need be considered.

Except for stars, all but a negligible fraction of the particles in the atmosphere have residual ranges longer than the dimensions of the chamber at 1-atm pressure. The diameter of the chamber is about 50 mg cm^{-2}. This is the

range of a 6-Mev proton, or a 0.1-Mev electron. The effect of the gas volume on star particles will be discussed below, and for all others, the actual chamber will be considered small enough to neglect interactions in the gas other than ionization.

The processes which will be considered are:

1) - Stopping of nuclear particles by the wall

2) - Production of nuclear shower particles

3) - Star production

4) - Electron showers, and their low-energy tail.

It is to be expected beforehand that stopping particles, and nuclear and electron showers will show small wall effect, because the wall is thin compared to the interaction length for these processes. The observed variation of the corresponding intensities with depth in the atmosphere can be used to see how small.

Fast particles passing through the chamber without interacting will be assumed to have no wall effect. Such particles would only lose energy by ionization at a constant rate, and the assumption states that any possible influence of the wall on them in a chamber of the size used will be neglected.

B. Penetrating particles

First, the low energy primaries which get in only at the pole are not stopped by the wall to an appreciable extent. Since absorption only is important, $\frac{1}{2}$ gm cm^{-2} of air will

stop as many particles as the $\frac{1}{2}$ gm cm^{-2} wall. The difference between the observed ionization at $\lambda_m = 88^\circ$, and at $\lambda_m = 56^\circ$ is 45 ions, if both are measured at 10 gm cm^{-2}. The corresponding difference at 20 gm cm^{-2} is 32 ions. The total ionization is 450-500 ions. 10 gm cm^{-2} greater depth corresponds to more than 10 gm cm^{-2} added path because of the non-vertical radiation. One concludes that the wall stops less than 1 in 100 of these low energy particles. Expressed as a fraction of total ionization, it is 1 in 1500.

The wall influences the protonic flux by nuclear interactions, and also by ionization loss. The collision length in iron for a proton is near 100 gm cm^{-2}. Therefore, 1 proton in 200 will suffer an encounter in the wall. We will put aside for the moment discussing the low energy star prongs, and confine ourselves to fast secondaries. The resulting interaction stops the original particle, and may produce one or more secondary particles of lower energy. The number of secondary particles, on the average, increases with the energy of the primary.

Since the wall is thin, we can write:

$$\Delta N_p = \frac{dN_p}{dt} \Delta t + \frac{dN_p}{d\tau} \frac{\Delta t}{\lambda} \qquad (18)$$

where,

ΔN_p = The change in total protonic flux caused by a thickness Δt gm cm^{-2} of material in the direction of the flux.

$\frac{dN_p}{dt}$ = The change in flux due to ionization loss, per gm cm^{-2}.

$\frac{dN_p}{d\tau}$ = The change in flux due to nuclear interactions, per interaction length.

Δt = The wall thickness.

t and τ are both measures of the same quantity, but in a different unit, t is in gm cm^{-2}; τ in interaction lengths. $\tau = \frac{t}{\lambda}$. The reason for introducing τ is to make the quantity $\frac{dN_p}{d\tau}$ independent of material. Since the nature of a nuclear reaction does not change rapidly with Z, they will be assumed to be similar in all materials considered. The number of reactions does depend on Z, and is taken care of by expressing distance in terms of interaction lengths. Ionization loss is independent of material to an adequate degree if distance is in units of gm cm^{-2}.

If $\frac{dN_p}{dt}$ and $\frac{dN_p}{d\tau}$ do not depend on material, their size can be estimated from the observed effect of a layer of air. The production of nuclear secondaries should be greatest at the top of the atmosphere near the equator. There, primaries all have energies much higher than the ionization loss in travelling one interaction length. Stopping by ionization can

be neglected, and the observed rate of increase of flux will be the maximum rate of multiplication of nuclear particles which could be observed anywhere. Komori (7) shows an average increase of 1% per gm cm^{-2} of air, for the total proton flux between 20 and 40 gm cm^{-2}, at $\lambda_m = 3^o$. The greatest absorption that could result from nuclear effects would occur if each interaction stopped the incident particle and produced no secondaries at all. The limits thus imposed are:

$$-1 < \frac{\frac{dN_p}{d\tau}}{N_p} < +0.65$$

The fastest observed attenuation of the total nuclear flux occurs at the higher latitudes. At $\lambda_m = 56^o$, $\frac{\Delta N_p}{N_p} = -0.008$ in a thickness of 1 gm cm^{-2}. If this is put into equation 18, along with the limits on $\frac{dN_p}{d\tau}$:

$$-0.02 < \frac{\frac{dN_p}{dt}}{N_p} < 0$$

$\frac{dN_p}{dt} < 0$ always, as no new particles can be made by ionization loss.

If these numbers are applied to $\frac{1}{2}$ gm cm^{-2} of iron, $\tau = 0.005$, using equation 18, the extreme values that can be obtained are,

$$-0.015 < \frac{\Delta N_p}{N_p} < +0.003$$

The lower limit results from the rather unlikely combination of enough particles stopping per gm cm^{-2} to offset the maximum rate of secondary particle production which could be observed anywhere, coupled with no actual secondary production. If this were actually happening at $\lambda_m = 56^o$, $\frac{\Delta N_p}{N_p} = -0.03$ per gm cm^{-2} in the air would result from equation 18 instead of the observed 0.01. Therefore, the actual wall effect must be considerably less than the above limit.

Heavier particles than protons have not been considered, but their relatively minor importance, ~10% of the total ionization at 10 gm cm^{-2}, makes their effect negligible. Mu mesons have been ignored also, as their average energy in the atmosphere is clearly too high for the walls to stop them. Their production would not be affected by the thin wall.

It is seen that no significant wall effect due to nuclear particles occurs if measurements no more accurate than 1% are contemplated. Other uncertainties will be much more important than this one.

C. Stars

The remaining processes, namely, the low-energy products of nuclear reactions and electron showers, were treated in more detail. These were expected to be the significant effects, and an attempt was made to get limits on the wall effect from them.

An analysis was made which applies to a small chamber. It was done without reference to any specific process, in terms of a production rate of secondaries and the rate of energy loss of these secondaries. If their range is less than the wall thickness, assuming an infinite medium surrounding the small chamber is justified. The results will enable one to evaluate the ionization which would be produced by star particles, for example, with the penetrating primary radiation held constant, if different materials surround the chamber. The difference between iron and air surrounding it will be the desired wall effect.

Say that an ionization is caused only by secondary particles whose production rate does not depend on position over a distance longer than either their range or the thickness of the instrument. First, assume secondaries are projected only in one direction and are not scattered, and then generalize to include the case of stars or electrons.

Let $P(E_o)$ = Production rate of secondaries at E_o, per unit volume and energy interval. P can depend on material.

$N(E)$ = Flux at energy E at the chamber.

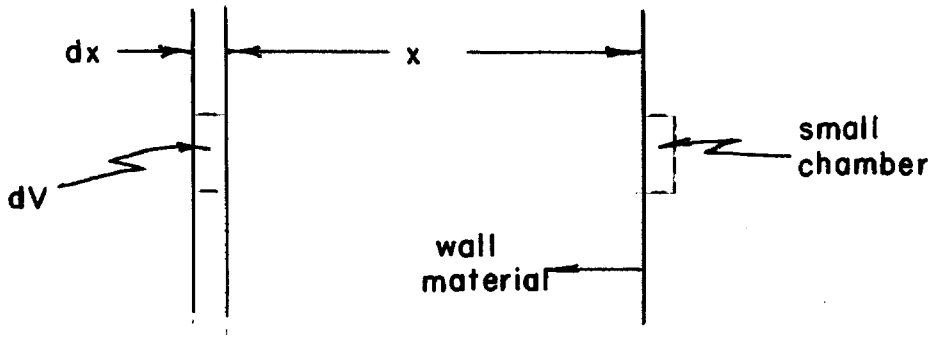

E_o is related to x and E by the range integral,

$$x = \int_E^{E_o} \frac{dE'}{\frac{dE'}{dx}} \tag{19}$$

E_o is to be understood as the energy at which a particle must be produced at distance x in order to arrive at x = 0 at energy E. We have:

$$N(E) = \int_o^\infty P(E_o) \frac{dE_o}{dE} dx \tag{20}$$

$\frac{dE_o}{dE}$ is required because particles produced in dE_o arrive at x = 0 in dE, which is not in general the same. If we write $\frac{dE}{dx} = \epsilon(E)$, and transform the integral to one on E_o,

$$N(E) = \int_E^\infty \frac{P(E_o)\, dE_o}{\epsilon(E)} \tag{21}$$

Actually, the production is not restricted to one direction. For infinite walls of one material, direction would only enter in generalizing $P(E_o)$, so,

$$N(E,\bar{r}) = \int_E^\infty \frac{P(E_o,\bar{r})\, dE_o}{\epsilon(E)} \tag{22}$$

It is now seen that density of the material is not a factor,

since P and ϵ are both linearly proportional to density.

To find the ionization, note the expression

$$I = \int_0^\infty J\sigma \quad dE \tag{23}$$

where J = omni-directional flux, $\int_{4\pi} N(E,\bar{r})\, d\omega$

σ = Specific ionization, a function of E.

The idea of a small chamber has been used here, by considering J only a function of E. More generally, it could depend on the position in the chamber, and should be integrated over the volume of the chamber. From equation 23,

$$I = \int_{4\pi}\int_0^\infty N(E,\bar{r})\ \frac{\epsilon_{gas}(E)}{w}\ d\omega dE \tag{24}$$

w is the energy to form an ion pair.

$$I = \int_{4\pi}\int_E^\infty\int_0^\infty \frac{P(E_0,\bar{r})}{w}\ \frac{\epsilon_{gas}(E)}{\epsilon(E)}\ d\omega\, dE_0\, dE \tag{25}$$

Elastic scattering of the particles, if electrons, does not affect the results, because it is the integrated flux which is significant. Scattering changes only the direction of the particle and not the energy. $\int_{4\pi} N(E,\bar{r})\, d\omega$ is not changed.

To apply expression 25 to the case of star evaporation particles, consider first the nature of $P(E_o)$. The data are from photographic emulsions, but do indicate that the form of $P(E_o)$ is not strongly dependent on Z. However, the magnitude of P depends on the material in accordance with the geometrical size of the nuclei. For the lighter elements, somewhat over half theprongs are α particles, the rest mostly protons. Their angular distribution is isotropic. The energy of the protons averages about 10 Mev, and for the α's, 15 Mev. For the accuracy necessary, it will be sufficient to assume all star prongs made by the same kind of particle have the average energy initially. Under these assumptions, expression 25 for the ionization becomes:

$$I = \int_0^{E_o} \frac{P_w}{w} \frac{\epsilon_{gas}(E)}{\epsilon_w(E)} \, dE \qquad (26)$$

The actual chamber wall is thicker than the range of star particles, so the assumption of an infinite wall is a good one. However, the 1 atm of argon 12 cm in radius is not a small volume, especially for the α's. In principle the ionization in the actual chamber could be calculated, in detail, knowing the quantities going into equation 25, but since no great accuracy is necessary, limits were obtained in the following way.

The small chamber ionization in argon can be calculated using expression 26, if it is surrounded by iron or argon or

air. The difference between the first two is not large, compared to the difference between the iron and air wall. In the actual chamber, a small central volume is surrounded by more argon to a radius of 20 mg cm^{-2}, and outside of this is the iron. In this situation, the ionization in the small central volume would be somewhere between what it would be with either all iron or all argon surrounding it.

Actually, the average ionization in all the chamber gas is measured, not just that at the center, but this must also lie between the extremes noted. Consider for a moment the flux $N(E,\bar{r})$ at some point in the gas. The particles have either followed a path wholly in the gas, in which case the flux (and ionization) is characteristic of argon: wholly in the iron, where the flux would be characteristic of iron; or partly in each, with an intermediate value of flux.

From the expression for ionization (equation 26) the value of I_{wall}/I_{air} can be written. The subscripts refer to the material surrounding the small chamber. "Wall" is either argon or iron.

$$\frac{I_{wall}}{I_{air}} = \frac{\int_0^{E_o} \frac{P_{wall}}{w} \frac{\epsilon_A}{\epsilon_{wall}} dE}{\int_0^{E_o} \frac{P_{air}}{w} \frac{\epsilon_A}{\epsilon_{air}} dE} \qquad (27)$$

Since $\frac{\epsilon_A}{\epsilon_{air}}$ is nearly ($\pm$ 10%) a constant,

$$\frac{I_{wall}}{I_{air}} \simeq \frac{P_{wall}}{P_{air}} \left(\frac{\epsilon_{air}}{\epsilon_{wall}}\right)_{av} \tag{28}$$

$$\left(\frac{\epsilon_{air}}{\epsilon_{wall}}\right)_{av} = \frac{1}{E_0} \int_0^{E_0} \frac{\epsilon_{air}}{\epsilon_{wall}} \, dE \tag{29}$$

The form of $\frac{\epsilon_{air}}{\epsilon_{Fe}}$ and $\frac{\epsilon_{air}}{\epsilon_A}$ is shown in Fig. 13. At low energies, 0 - 2 Mev, the experimental data summarized by Fuchs and Whaling (28) were used, and for 5-10 Mev, Aron's (29) tables. The curves are for protons. The same ones were used, in the lack of any better information, for the α particles, with the energy scale properly altered. The relative production rate was assumed to be in the same ratio as the geometrical size of the respective nuclei.

Applying the curves in Fig. 13 in equation 28, first for 10-Mev protons, and then for 15-Mev α particles, the following values of I_{wall}/I_{air} result.

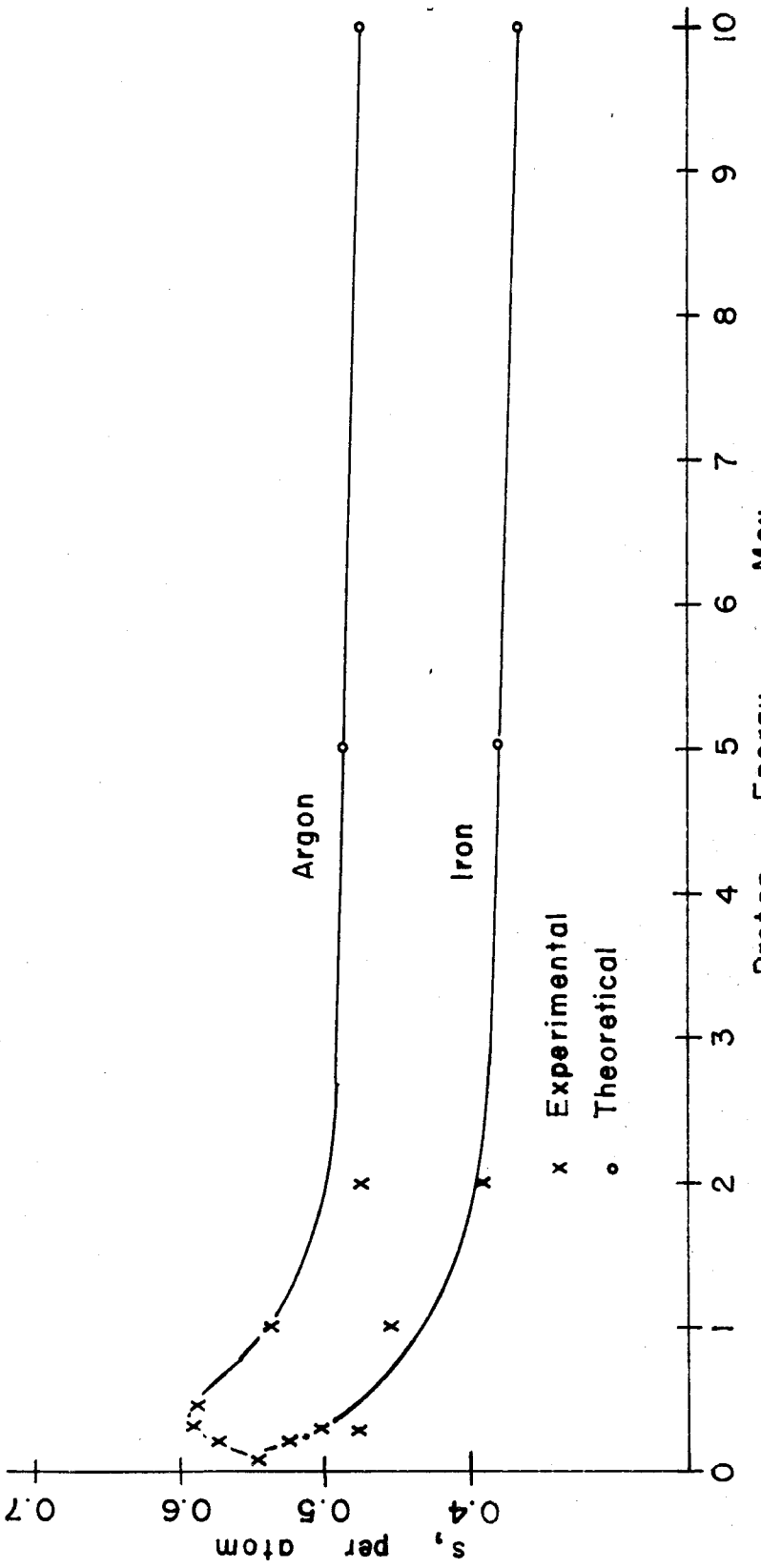

Fig. 13 $s, (dE/dx)_{air}/(dE/dx)_A$ or Fe, vs proton energy. s is in units of relative energy lost per atom.

	Fe wall	Argon wall
protons	0.96	0.96
α particles	1.03	1.02

It is clear that no great error will be made by using the small chamber idea, even though the actual chamber is not small.

The most probable $\frac{I_{Fe}}{I_{air}}$ for the whole star is 1.01. The probable error of such an estimate will be of the order of 10%. Star ionization is 8% of the total ionization in the range of altitude considered, so the wall effect due to stars is $0.0 \pm 0.8\%$ of the total.

D. The electronic component

The electronic component is affected by a number of competing processes. Pair production, Compton, and photo-electric events can produce secondary electrons. Brem-strahlung and ionization losses absorb them. The relative importance of these processes, of course, depends on the energy considered. To afford a reasonably simple treatment, a division was made separating the radiative and non-radiative processes. Electrons and photons with energy greaterthan the critical energy for iron were assumed to multiply by the shower process in the wall. Electrons produced in the iron with less than the critical energy were assumed to be pro-duced by the Compton effect, and to lose energy by ionization only.

The following approximations will be made to make possible an estimate of the size of the shower transition in the thin iron wall. An electron with more than the critical energy will be assumed to produce a photon of half its original energy with unit probability per radiation length. A photon with more than the critical energy will be assumed to divide its energy equally between the positive and negative electron. The actual pair production probability in iron per radiation length was used. Energy loss is neglected for energies greater than critical. This model and its general consequences are discussed by Rossi (30). The thickness of the iron wall is 0.04 radiation units. Since it is so thin, the chance of a photon produced in the iron in turn producing an electron pair is nil. Therefore all electrons with energy greater than the critical energy pass through the chamber wall, although 4% of them have lost half their energy. Photons will produce 2 electrons in each interaction, and the two electrons will always cross the gas, according to the approximation being employed.

Unfortunately, the electron energy spectrum has not been measured at very low energy or high altitude. The track-length spectrum of shower electrons and photons has been computed by Richards and Nordheim (31) down to a 4 Mev, including all the important effects. It agrees in form with some measurements at sea level and 600 gm cm^{-2} by Barker (32), and also with those of Greisen (33) at sea level. The form of the

track-length spectrum with some of the experimental points, fitted at 10 Mev, is shown in Fig. 14. The experimental spectrum is not altitude dependent between 600 gm cm^{-2} and sea level. One would expect it to be similar at 100 gm cm^{-2}, since most showers are fully developed there, and the electronic intensity is at a broad peak. However, at 10 gm cm^{-2}, the track-length spectrum may not correctly represent the actual spectrum.

If the electron and photon energy distribution incident on the chamber is that of Richards and Nordheim, the increase in flux of electrons with energy greater than the critical energy in iron can easily be computed using the model mentioned above. The result is an increase in the total ionization at 100 gm cm^{-2} of $\sim$2%. Since energy loss by ionization has been neglected, the result is an overestimate. If a similar calculation were made for air, an increase of 1% would be obtained. Actually a slight decrease is observed. Therefore the shower multiplication process in the wall can be neglected without serious error.

At higher altitudes, the electronic component is multiplying extremely fast in air, and can be expected to increase even faster in iron. An increase in the number of electrons of over 5% in the wall may be expected at the highest altitudes. However, since only 10% of the total ionization is due to electrons at 10 gm cm^{-2}, no significant error in the total ionization will occur.

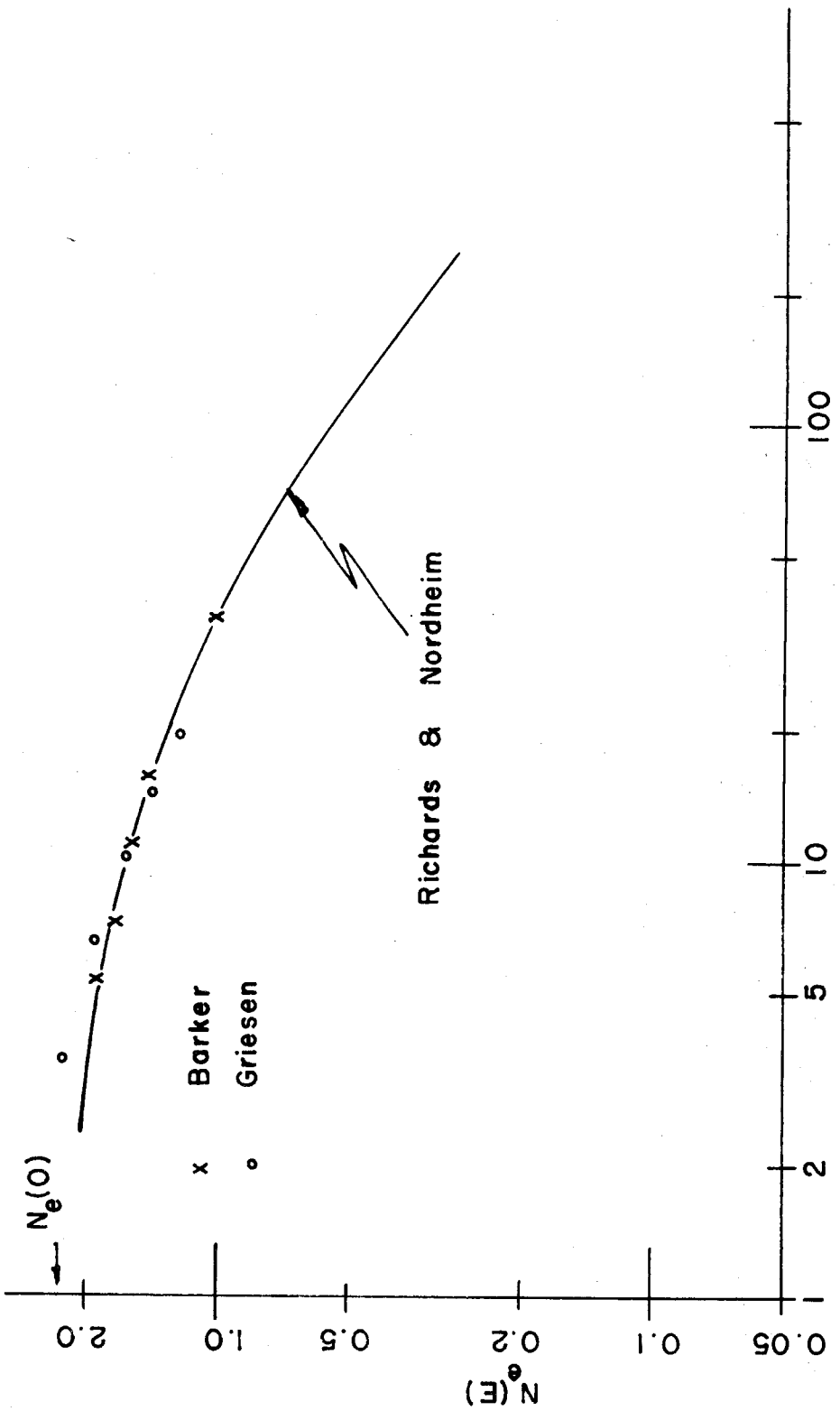

Fig. 14 The theoretical integral track-length spectrum of Richards and Nordheim, compared to some experimental points.

The low-energy electrons need only be considered at 100 gm cm^{-2}, because both the fraction of the total intensity in the electronic component and the incompletely developed showers tend to make their influence less at higher altitudes. We have already assumed that electrons and photons below the critical energy for iron do not undergo shower multiplication. The further assumption will be made that all the electrons produced below 10 Mev are produced in the iron, to make sure that an overestimate of the wall effect is being obtained. The range of a 10-Mev electron is about 10 times the wall thickness, so by no means all of them are actually produced in the wall. A complete transition does not actually occur.

The spectrum of Richards and Nordheim was extended below 4 Mev by noting that the total integral track length was known because the total energy of the shower is given. The exact form is not important; only the number of electrons below 10 Mev. However, the photoelectric effect is important below $\sim$200 Kev, and so the number of electrons in this interval is also desired. In Fig. 15, the differential energy spectrum of Richards and Nordheim is plotted down to 4 Mev, and the average below 4 Mev needed to give the proper integral is dotted in. There cannot be an infinite peak at E = 0 because of the increasing ionization loss. If the spectrum is arbitrarily extended in the straight line shown, the integral of the flux below E = 200 Kev is 1% of the total

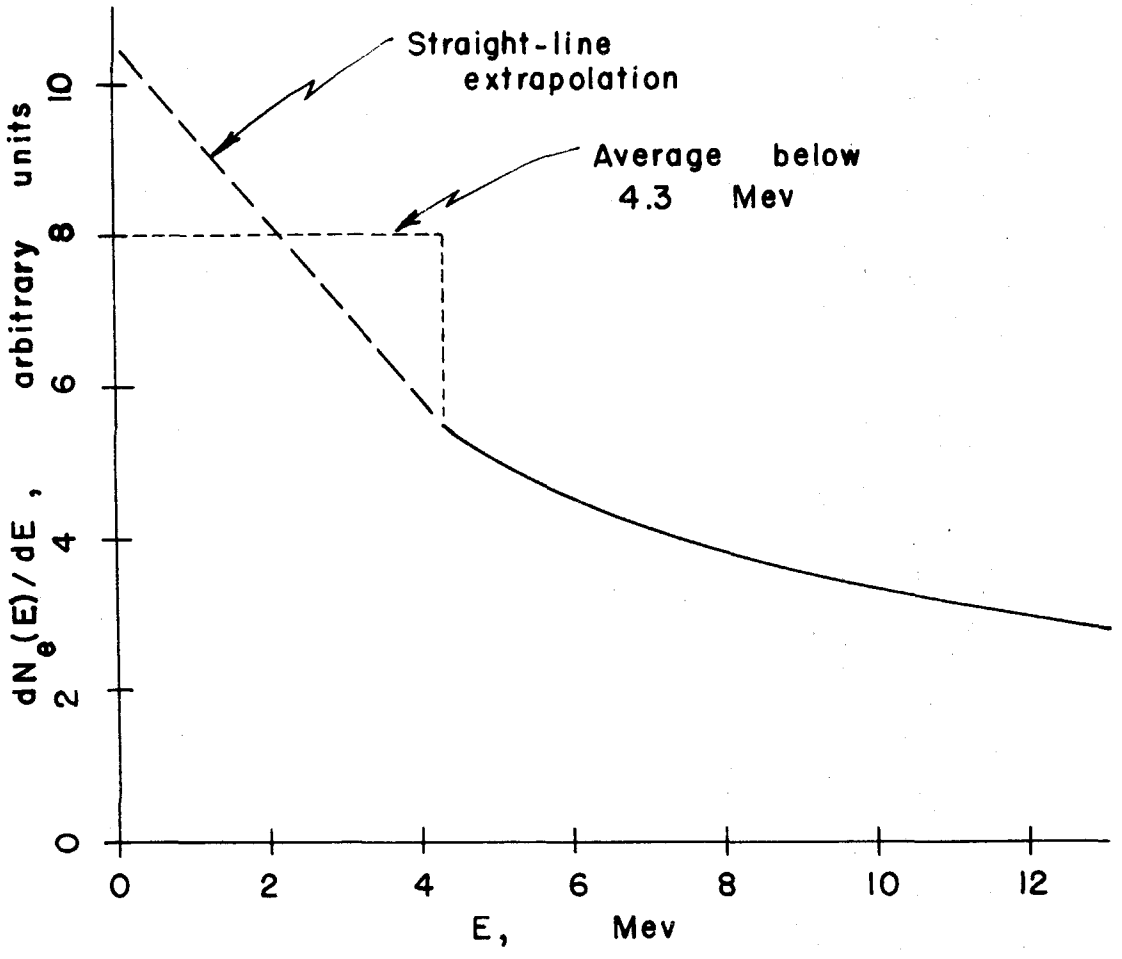

Fig. 15 The differential track-length spectrum of electrons at low energies. The total number of particles below 4.3 Mev is fixed because the total energy of the shower is given.

electronic flux. It would be very difficult, if not impossible, to invent a reasonably continuous extension of the track-length curve, with the proper integral, which would put 5% of the total number of electrons below 200 Kev. On this basis, neglect photoelectrons.

The wall effect by electrons of less than 10 Mev energy was estimated by the same analysis used for the star particle wall effect. Consider only one direction in equation 25, since any direction is representative. Since all electrons below 10 Mev are assumed to be produced in the wall by Compton effect,

$$I = \int_E^{10} \int_0^{10} \frac{P_{wall}(E_0)}{W} \frac{\epsilon_{gas}(E)}{\epsilon_{wall}(E)} dE_0 dE \qquad (30)$$

To the accuracy needed, we can replace $\frac{\epsilon_{gas}}{\epsilon_{wall}}$ by hs, both constant, $h = \frac{\epsilon_{gas}}{\epsilon_{Air}}$: $s = \frac{\epsilon_{air}}{\epsilon_{Fe}}$. Using the same notation used earlier for star ionization,

$$\frac{I_{Fe}}{I_{air}} = \frac{\int_E^{10}\int_0^{10} \frac{P_{Fe}(E_0)}{W} hs \, dE_0 dE}{\int_E^{10}\int_0^{10} \frac{P_{air}(E_0)}{W} h \, dE_0 dE} \qquad (31)$$

Since P depends only on electron density in the Compton effect,

$$\frac{I_{Fe}}{I_{air}} = s \,, \tag{32}$$

if s is expressed in energy loss per electron. From tables by Aron (29), s = 1.15 (for 1-Mev electrons). Consulting the electron energy spectrum, and Fig. 11, this result implies a wall effect of 2.7%, expressed as a percentage of the total ionization. Note again that this is an upper limit, and that it is based on an assumed spectrum, and will be in error in proportion to the error in the spectrum.

A lower limit might be obtained by looking at the number of electrons below 2 Mev, which certainly are produced in the wall, but the result is not significantly bigger than zero. A lower limit of zero will also apply at higher altitude, because no process seems to make a negative wall effect; that is, more ionization without the wall.

This result will be combined later with other quantities whose uncertainties are expressed in the form of a statistical error. Therefore, the most probable electron wall effect will be rather arbitrarily set halfway between the two limits, and the probable error will be set equal to half the difference. That is, the electron wall effect is $1.4 \pm 1.4\%$.

To summarize the wall effect estimate, the protonic component was not found to be influenced appreciably by the wall, either by stopping or by nuclear showers. The low energy star particles from nuclear reactions do produce about 1/10 of the total ionization, though, and since their ranges are about the wall thickness, they were expected to contribute a wall effect. However, it turned out that in terms of the total ionization, the wall effect from stars was $0.0 \pm 0.8\%$, a small effect.

The electronic component was also expected to contribute, due to the large number of low energy electrons, and because of the influence of shower development for high energies. An estimate was made for 100 gm cm^{-2} depth, and it was found that showers were not an important effect, but that low energy secondaries might be. Limits were obtained for the wall effect using a spectrum extrapolated to zero energy on the basis of shower track length calculations. The result was $W.E._{electrons}$ $1.4 \pm 1.4\%$. The situation at higher altitudes was also examined. The showers were found to increase in importance with altitude, but the total effect was covered by this estimate because the total number of electrons is much less.

VI. COMPARISON OF CHAMBERS AT 1 AND 8 atm PRESSURE

A. The experiment

Two flights were made in the summer of 1955 at Thule, Greenland, with a chamber filled to 1 atm. Two instruments were attached to the same balloon in each case, one the normal 8-atm one, and the other filled to 1 atm. This enabled the results to be compared directly, with no error from altitude or fluctuation in cosmic-ray intensity possible. Immediately before the flight, both instruments were calibrated in the set-up described previously.

The 1-atm chambers were identical to the 8-atm ones, except that the gas was released immediately before the flight, and the filling tube resealed. The resulting pressure was approximately the atmospheric pressure existing at the time, but it was not measured.

No complications arose from the lowered pressure, except that the resulting time between discharges was 8 times longer, or about 2 minutes at the top of the flight. A small amount of noise picked up in the recording equipment could render the record undecipherable. To prevent this, one of the transmitters was altered, so that it would transmit about 4 pulses spaced about 1/5 sec at each discharge of the chamber. However, no change was made on the second flight, and no difficulty was encountered.

The results of one of these flights are represented in

Fig. 16, in terms of I_o, meaning that the constants used are the right ones to make the chambers indicate the same ionization in the calibration set-up. During the flight, in the range of depth for which data were obtained from both instruments, which was from 7 gm cm^{-2} to 140 gm cm^{-2}, they operated with the same ratio of currents as they did when compared on the ground, within about 1%.

B. Interpretation

In reality, the calibration set up, using gamma rays, produced 6% less ionization in the 8-atm chamber, meaning that 6% less ionization was being produced in it by the cosmic rays, too. As long as their response is proportional, data from chambers at either pressure may be reported in terms of ionization in the atmosphere as well as the other. No quantitative explanation of this difference was forthcoming but a number of causes can be put forward. The higher pressure gas suffers some recombination loss for the heavily ionizing star particles. The relativistic density effect causes less energy to be lost at the higher pressure by extremely fast particles. Wall effects show up as a pressure dependence of ionization. Finally, the energy, w, to form an ion pair may change with pressure.

The recombination loss was computed in Chapter IV for a chamber at 8 atm pressure. As data from a pulse ion chamber were used, the results may be somewhat too big, but an integrating chamber indicated a similar situation. The conclusion

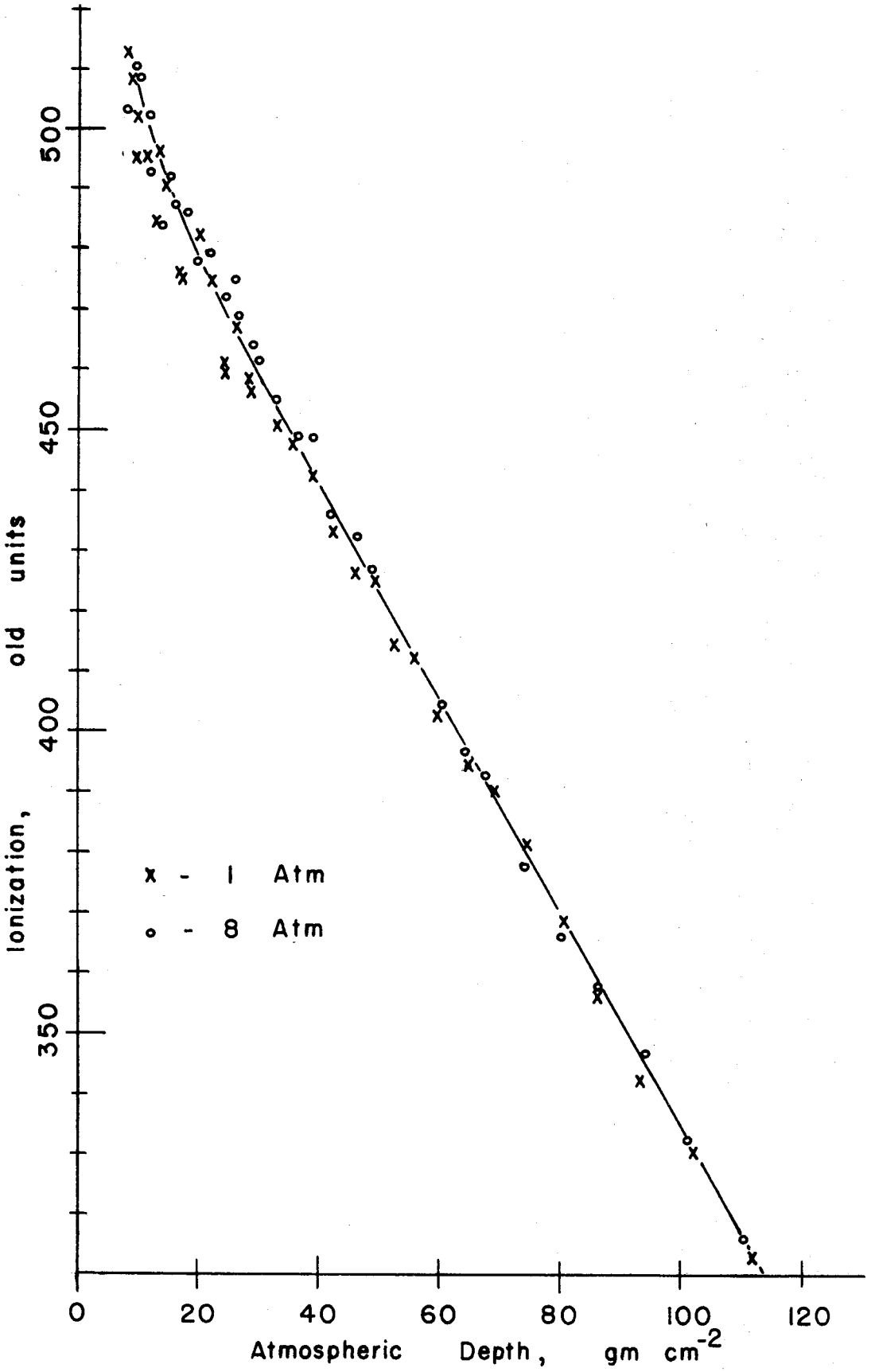

Fig. 16 Results of a flight with two instruments, at Thule, Aug 7, 1955.

was that columnar recombination was an important effect, due to the low fields existing near the outside of the chamber. About 3% loss of the total ionization can be expected. The loss will occur over the entire range of altitude for which data were obtained, but will tend to be somewhat greater at the top due to heavy primaries.

The difference in ionization due to the density effect was computed for 100 gm cm^{-2} depth by Fermi's (34) formula for the density correction to the energy loss, and the same electronic energy spectrum used before (Fig. 14). The general behavior that shows up is thatthe rate of energy loss levels off, as E increases, at different values for different densities. The difference increases fairly rapidly above a certain energy, to a constant value, which remains to infinite energy.

There may be some question about what the density correction really looks like, but this general picture is not affected much. The velocity at which $\frac{dE}{dx}$ begins to depend on density may be somewhat in question.

$$\frac{\frac{dE}{dx}(1\ atm) - \frac{dE}{dx}(8\ atm)}{\frac{dE}{dx}(1\ atm)} = \begin{cases} .06 & E \text{ (for electrons)} > 30 \text{ Mev} \\ 0 & E \leq 30 \text{ Mev} \end{cases}$$

is a suitable approximation. The corresponding energy for μ mesons is 15 Bev, so their effect will be neglected.

The difference in total ionization can be obtained from this, Fig. 11, equation 34, and Fig. 14, assuming the energy

to form an ion pair is comparatively constant. The result is a drop in ionization observed in a chamber at 8 atm pressure of 1.3%, compared to a similar chamber at 1 atm. At 10 gm cm^{-2}, the drop would be half this, even if all the electrons present according to Fig. 11 had energies above 30 Mev. Therefore, the difference can be expected to diminish considerably at the highest altitudes, partly compensating for the increase in recombination.

The exact way that wall effect shows up as a function of pressure is difficult to estimate. Since it is only the partial transition in the added gas that depends on pressure, the effect of the chamber wall discussed in the last section may be expected to be larger. The wall is not likely to contribute more than 1% to the observed variation of ionization with pressure.

The energy to form an ion pair, w, may possibly depend on pressure, but the form of the dependence is not known. An experiment was made of putting some Po^{210} on a small disk attached to the central electrode (Fig. 1), and varying the pressure. The ionization dropped 2% at the 8 atm pressure, compared to what it was at 1 atm. This represents the degree of variation of w if all ions were being collected, or if an equal fraction was being collected. Corrections were made to approach this situation.

The total of these estimates is 7% difference between the two pressures. The agreement isnot as good as desired,

since the 7% is a sum of upper limits. However, it does indicate that the processes considered can account for a difference of the order of the one observed. The view is taken that the effect is in fact due to the processes mentioned, and that if an accurate accounting could be made, it would explain the experimental results.

VII. THE RELATIVE IONIZATION IN ARGON AND AIR

A. The data

The ionization produced in an argon chamber has been obtained, and the effect of the chamber wall has been estimated. The resulting "small chamber" ionization can now be converted to ionization in the air by knowing the ratio of ionization in the two gases by the particles present in the atmosphere.

The measurements of I_{air}/I_A available were the present one, made with a 25 cm diameter chamber using Th C" gamma rays; Bakker and Segre's (35) for 340-Mev protons; and Cox's (36) for gamma rays in a chamber with small free volume. The present result was 0.665, with an error of 1%. For 340-Mev protons the value of 0.685 resulted, with an error estimated at 2-3%. The chambers used with the protons were thin walled (foil) and were disc shaped, with the proton flux passing through axially. Some effort was made to eliminate recombination, and the gases were the ordinary tank gases available at the time. Cox obtained 0.71 using a chamber which had a free volume about 1 cm thick by 10 cm in diameter. Cox also used tank gases, but at the time of his work, the argon was considerably less pure than it is now, and therefore there may be some uncertainty in comparing his values with more recent ones. Also, an experiment was tried here

using a very small chamber, which verified that $\frac{I'_{air}}{I'_A}$ (γ) is larger than it is in a big chamber.

The ratio of particle ionization in air and argon is given by the relation:

$$\frac{I_{air}}{I_A} = \frac{\left(\frac{dE}{dx}\right)_{air}}{\left(\frac{dE}{dx}\right)_A} \frac{W_A}{W_{air}} = S\frac{W_A}{W_{air}} \qquad (34)$$

where w = the energy to form an ion pair.

The values used for w have been independently obtained by a number of methods. A summary of some experimental values in argon and air is shown in Tables 4 and 5, and the method used is noted. The values have been averaged without regard to the method used, or the accuracy of the experiment. The resulting average value, and the probable error resulting from the averaging process are shown. The individual determination with the best quoted experimental error is compared to the average. The ratio w_A/w_{air} using the two averages is 0.770. Bakker and Segre's absolute values are somewhat low due to nuclear interactions, but their ratio agrees with the average.

The evidence seems to indicate that with care, a fairly good value (1 - 2 %) can be obtained. The effects to look out for are a lack of saturation for α's in air (37), and impurity in the argon. The recent results of Jesse and Sadauskis (38)

Table 4

Summary of Some Experimental Determinations of w in Argon

Ref	Experimenter	Method	w, ev
36	Bakker, Segre	340-Mev protons	25.5
44	Jesse	Po α's in pure gas	26.4 $\pm$ 0.2
45	Frost, Nielsen	Experimental specific ionization and theoretical dE/dx at min ionization for electrons	27.9 $\pm$ 1.5
46	Weiss, Bernstein	2-Mev electrons	25.5 $\pm$ 0.3
47	Valentine	Po α's	26.9
		A^{37}, with a β activity at about 2 Kev mixed in the gas in small quantity	27.0
48	Sharpe	Pu α's	26.3
49	Haeberli et al.	Po α's	26.25
		Average value	26.3 $\pm$ 0.2
		Best single determination (Jesse)	26.4 $\pm$ 0.2

Table 5

Summary of Some of the Experimental Determinations of w in Air

Ref	Experimenter	Method	w, ev
36	Bakker, Segre	340-Mev protons	33.3
44	Jesse	Po α's: admits recombination	35.5
		Beta particles from Ni^{63}, about 15-20 Kev	34.1 ± 0.3
45	Frost, Nielsen	Experimental Specific ionization and theoretical dE/dx at min ionization for electrons	31.2 ± 1.5
46	Weiss, Bernstein	2-Mev electrons	33.9 ± 0.8
47	Valentine	Small amount of A^{37} in the gas. The absolute determination was in argon	35.0
		Po α's	35.2
48	Sharpe	Pu α's	35.6
43	Alder et al.	Po α's, very high fields	34.7 ± 0.5
		Average value	34.3 ± 0.3
		Best single determination (Alder et al.) (Jesse)	34.7 ± 0.5 34.1 ± 0.3

for the effects of impurity in helium are alarming, but the impurities that affect argon are more limited (to ones with quite low ionization potential), and the size of the effect observed in argon was quite a bit smaller than the one in helium. Apparently only 2/3 of the energy dissipated in the gas appears in ion formation. The rest goes into excited states and photons. The balance between the fraction appearing as ions and the non-ionizing part can be affected by small amounts of impurity. The modern gas is claimed by the manufacturer to be purer by a factor of 10 than the amounts of impurity Jesse was talking about (1 in 10^4).

When gamma rays are used to produce the ionization, I_{air}/I_A can be expected to vary with the size of the chamber. The ratio of energy absorbed in the two gases from electrons ejected from the wall will be somewhat different than that for photons. The energy absorbed from a photon is proportional to NZ, the number of electrons per cm^3, if it only suffers Compton encounters. If photoelectric absorption does occur there will be a stronger dependence on Z. If the gas volume is large compared to the range of the secondary electrons, the relative ionization will be given by the rate of absorption of energy from photons,

$$\frac{I_{air}}{I_A} = \frac{NZ_{air}}{NZ_A} \quad \frac{W_A}{W_{air}} \tag{35}$$

$NZ_{air}/NZ_A = \frac{14.5}{18}$, so $I_{air}/I_A = 0.62$, if w_A/w_{air} is taken as 0.770. From the expected amount of photoelectric ionization, I_{air}/I_A should actually be 0.55 or 0.60.

The value of I_{air}/I_A to be expected for particles can be obtained in the same way that it was estimated for gamma rays. The result will be more accurate, because there are no competing processes to worry about. From Fig. 17, the value of s is 0.89, for either 340-Mev protons, or the electrons of $\sim\frac{1}{2}$ Mev average energy ejected from the wall by Th C". Therefore,

$$\frac{I_{air}}{I_A} = 0.89 \times 0.720 = 0.685$$

This is in agreement with Bakker and Segre's value, and with Cox's, within the accuracy to be expected. It does not agree with 0.655. An explanation based on the production of secondary electrons in the gas is available.

The observed value of I_{air}/I_A using gamma rays lies between the expected value for gamma rays absorbed in the gas (0.60), and that for charged particles passing through (0.68). This implies a ratio between ionization produced by particles coming from the walls and those produced in the gas of 2:1. The observed value of $\frac{I'_{air}}{I'_A}(\gamma)$ in the 10" diameter chamber ought to be slightly different if the walls are changed, and contribute a significantly different part of the ionization. This is the case with the lead-tin wall. The value of

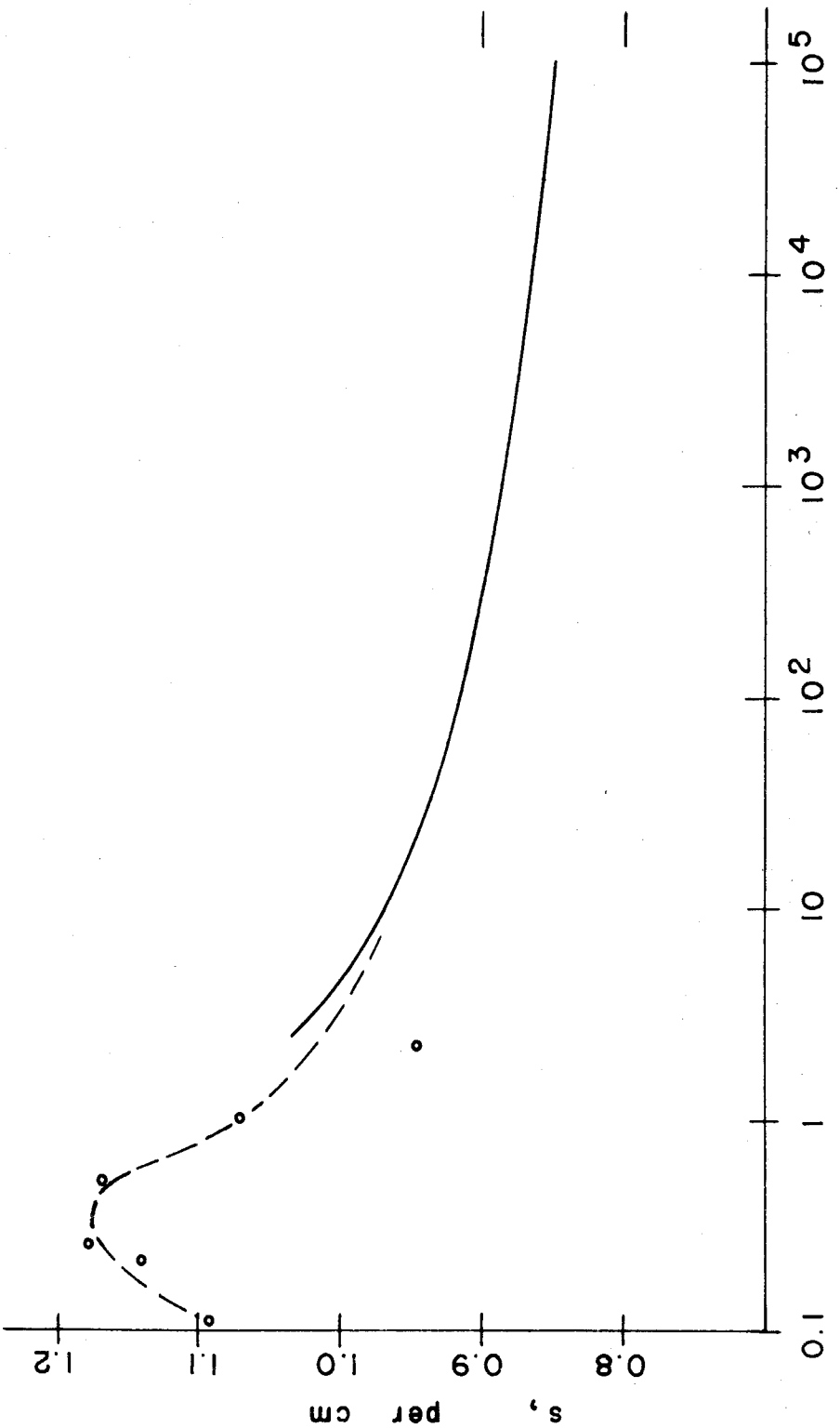
s, $(dE/dx)_{air}/(dE/dx)_A$, vs proton energy. s is the relative energy
lost per cm of gas. The solid line is from Aron's calculations, and
the dotted line is an extension to low energy on the basis of experi-
mental data.
s, per cm
0.8
0.9
1.0
1.1
1.2
0.1
1
10
10^2
10^3
10^4
10^5
E, Mev (for protons)

Fig. 17

did turn out to be larger by the correct amount when measured in the solder-coated chamber.

B. The effect of velocity

In view of the above discussion, the value of $\frac{I_{air}}{I_A}$ from Bakker and Segre is the correct one to use for fast particles. Segre (40) quotes 2-3% as the error of measurement. $\pm$ 2% will be used here on the strength of the agreement with the independent value from $S \frac{W_A}{W_{air}}$. Therefore, experimentally, $\frac{I_{air}}{I_A} = 0.685 \pm 0.014$, for particles with the velocity of a 340-Mev proton. This will be corrected for h class of particle present inthe atmosphere by the theoretical expression for the variation of s with velocity. Referring to equation 34; $\frac{I_{air}}{I_A} = S \frac{W_A}{W_{air}}$, the energy to form an ion pair does not show a velocity dependence in its experimental determinations. The value obtained using electrons is not systematically different from that obtained with α particles. The two kinds of particles used represent a very large range of velocity. In argon it is observed to be strictly independent of α particle energy. Some observers have found a dependence of w on α particle energy in air, but there is evidence to show that the reason is that saturation had not been obtained (37). A good discussion of the behavior of w has been made by Bethe and Ashkin (39). The relative quantity $\frac{W_A}{W_{air}}$ will be assumed independent of velocity. It will also be assumed independent of gas density as long as it is below 1 atm. A 2% or less variation in W_A was found in

going from 1 to 8 atm in an earlier section so $\frac{w_A}{w_{air}}$ might be expected to be constant, compared to s , at pressures below 1 atm. Assuming w_A/w_{air} constant means that the variation in $\frac{I_{air}}{I_A}$ becomes the same as the variation of the relative stopping power, s.

The quantity s is plotted in Fig. 17 to show the degree of its velocity dependence. It is expressed in terms of energy loss per cm. The solid line is from the tables of Aron, and comes from the theoretical energy loss expression. It is numerically accurate to 1%. Experimental points at low energies have been plotted and the probable extension of the theoretical curve is shown. s varies from 0.85 at 10^5 Mev (for Protons) to 1.15 at low energy. Since the variation with velocity is a result of the different values of I, the average ionization potential, and since the same I describes energy loss by electrons and heavy particles, with only small corrections being made to the total energy loss, the value of s shown applies to all particles of the same velocity.

The pressure of air at depths of 10 and 100 gm cm^{-2} is 1/100 and 1/10 atmosphere, respectively. The relativistic correction to the energy loss will enter into s, but at low densities like these, very large values of energy are required to bring the density effect into force. When the 1-and 8-atm chambers were compared it was discovered that the greatest difference in ionization will occur at the 100 gm cm^{-2} depth,

because electrons are the only effective particles. A similar estimate gives less than 1% density effect in going to the pressure outside the chamber, so it will be neglected in the following.

Except at very low energy, s varies 2-3% for a factor of 10 change in energy, a slow variation. For a given type particle, the important energy range is hardly twice this, so it is sufficient to say that the relative ionization of the protonic component, for example, is equal to the relative ionization for protons having the average energy. Due to the slow variation of s, a crude estimate of average energy is sufficient.

The energy spectrum of secondary protons in the atmosphere has been calculated by Rossi (41). Range phenomena cut it off at low energies, and the peak is at $\sim$100 Mev. The exact form, however, is sensitive to the assumed production spectrum. The average energy of the spectrum he gives, if extended to 10 Bev by a power law, is of the order of 1 Bev. Neher (3,9) gives an energy spectrum of primary particles derived from geomagnetic considerations. The average energy of this spectrum is of the order of 4 Bev, if extended to E = 0. If cut off below 1 Bev, the average energy will be about 6 Bev. At high latitudes, therefore, no significant errors will be made by taking the average proton energy at 3 Bev, at all altitudes considered.

The average meson energy in the atmosphere is of the order of a few Bev, corresponding to a proton energy of a few tens Bev. Since mesons are not abundant at balloon altitudes, their average energy does not need to be known very well. The π mesons are, of course, included in the protonic component, but they were neglected.

From the same spectrum used for computing the electronic wall effect, the average electron turns out to be 100-200 Mev corresponding to a proton energy 1800 times as big, or 2×10^5 ev.

Star particles have very low energy, and therefore their relative ionization will be way out of line. $3\frac{1}{2}$ Mev was used for their average energy, in terms of proton energy.

The variation of s with velocity from that of a 340-Mev proton is used to find the relative ionization for each type cosmic-ray particle, according to its average energy, $\langle E \rangle$. The resulting Δs, defined by $\Delta s = \frac{s(340) - s\langle E \rangle}{s(340)}$, along with the corresponding relative ionizations are:

$m_o c^2$	$E / m_o c^2$	Δs %	I_{air}/I_A
Protons	3	2.7%	.666
Mesons	2 x 10	4.7	.652
Electrons	4×10^2	6.3	.641
Stars	3×10^{-3}	-12	.77

These corrections are rather large compared to the errors of measurement. If theory can correctly describe the variation in relative stopping power, they are probably correct within 1%, which is smaller than the uncertainty in the experimental relative ionization for 340-Mev protons.

If Fig. 11 is consulted, an average value of I_{air}/I_A can be obtained for the total cosmic-ray radiation. This was done at 10 gm cm^{-2} and at 100 gm cm^{-2}, and the result was:

x, gm cm^{-2}	$\left\langle \frac{I_{air}}{I_A} \right\rangle_{av}$
10	0.672 ± 0.017
100	0.659 ± 0.017

The difference of 2% between the two levels is due to the varying proportion of protons and electrons, and not to a change in the average energies used.

Variations in the average particle energy with geomagnetic latitude would ordinarily not be expected to affect $\left\langle \frac{I_{air}}{I_A} \right\rangle_{av}$ significantly, because a large change in energy would be required. It should be kept in mind, however, that in extreme cases this is something which ought to be considered. For example, suppose an instrument was detecting mostly primary particles, near the top of the atmosphere at the equator. The primaries will be subject to a geomagnetic cutoff of the order of 10 Bev, and their average energy may be, say, three times that. Under these special conditions,

$\left\langle \frac{I_{air}}{I_N} \right\rangle_{air}$ could be 2% smaller than it would be at the same depth at the pole. The difference would be expected to diminish rapidly with altitude, as the high energy primaries tend to make more secondaries rather than proportionately higher energy ones.

VIII. SUMMARY AND CONCLUSIONS

A. Results

The results of this determination are summarized in Table 6. They are given in terms of I_o, the ionization which would be obtained using the existing calibration. The wall effect correction which was applied, and the ratio $\left\langle \frac{I_{air}}{I_A} \right\rangle_{AV}$ which was used are also shown. The results are given for two depths, 10 and 100 gm cm^2. The unit of I_{air} is ions cm^{-3} sec^{-1} atm^{-1} of air at 20°C.

The slight dependence of I/I_o on altitude is a result of the velocity dependence of the relative ionization by particles in air and argon. This variation is somewhat smaller than the uncertainty in the final result. A constant ratio;

$$I_{air}/I_o = 1.049 \pm 0.03$$

can be taken, and varies less than 1% from the one obtained at the limiting altitudes considered. Fig. 18 shows I_{air} and I_o on the same graph for easy comparison.

It is to be understood that I_{air} means ionization which can be collected in an ion chamber, from thin tracks, at a low level of ionization, in 1 atm of air, with reasonable collection voltages. By reasonable is meant low enough so that no fields exist in the chamber sufficient to cause mul-

Table 6

Summary of Results

		Depth gm cm^{-2} 10	100
1. Ionization in the 1 atm chamber in argon	$\frac{I'_A}{I_o}$	1.597±0.016	1.597±0.016
2. The wall effect correction in percent (subtract)		1.4 ±1.7	1.4 ±1.7
3. The factor to convert to ionization in air	$\frac{I_{air}}{I}$	0.672±0.017	0.659±0.017
4. Ionization in the air	$\frac{I_{air}}{I_o}$	1.058±0.031	1.040±0.031
Mean		1.049	

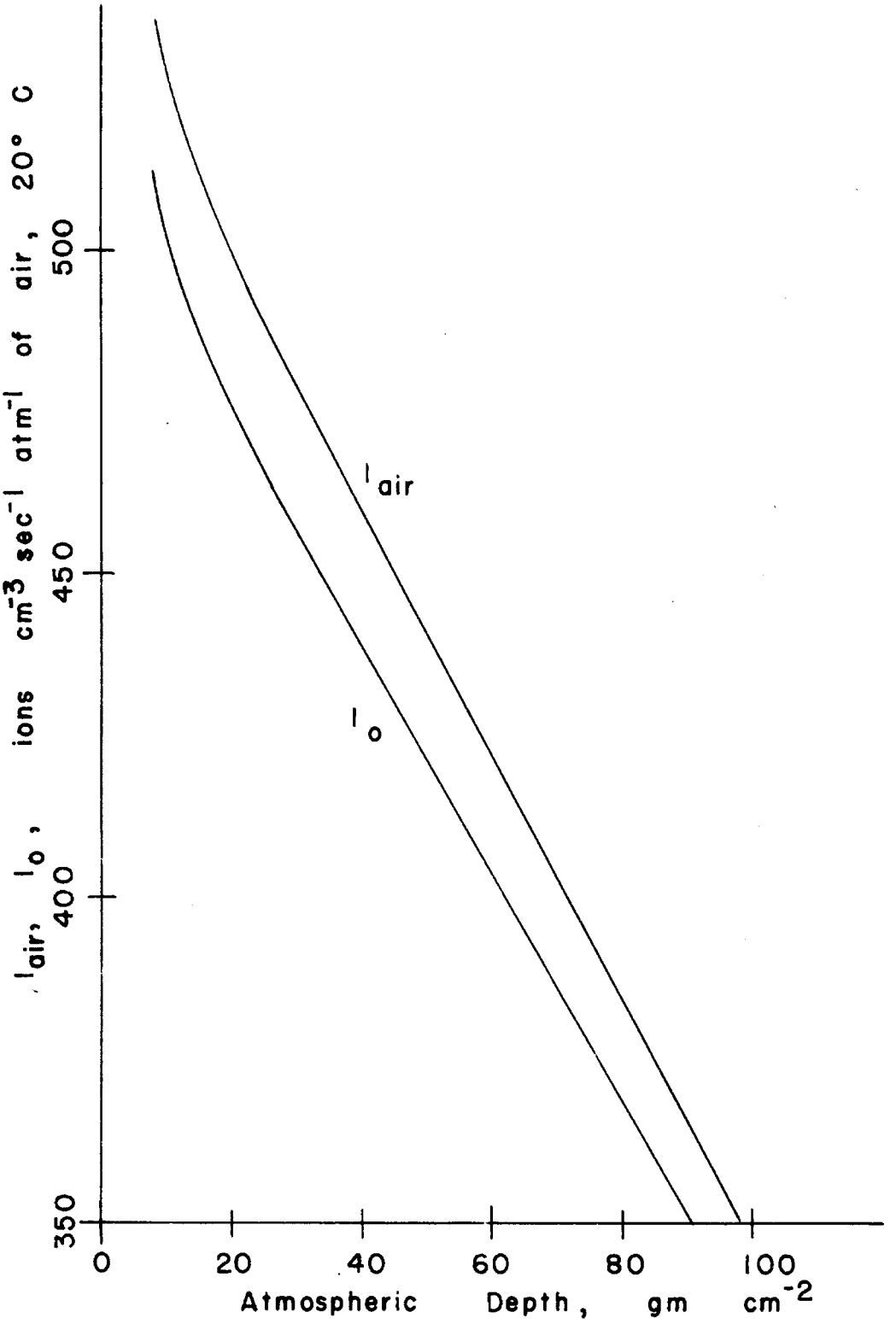

Fig. 18 I_{air}, the ionization according to this determination, compared to I_o, the ionization given by the existing calibration.

tiplication or breakdown.

It is assumed that all ions formed could be collected under these conditions. Whether or not this is strictly true is immaterial, because the same assumption is made when ionization is related to other physical quantities. The energy to form an ion pair is determined by ion chambers, and an ion must be collected to be counted. Specific ionization measured by cloud chambers has a similar requirement since an ion must stay an ion long enough to form a droplet.

The effect of recombination was eliminated by making the measurement in a chamber filled with 1 atm argon. The main uncertainties were in the wall effect correction, and in the value to use for the relative ionization by cosmic rays. The value for the ionization in the argon in the specific chamber used is believed accurate to 1%.

The wall effect is small because the wall is thin, but its exact estimation depends on the energy spectrum and behavior of the electronic component in the atmosphere. Estimates of other contributions to the wall effect indicate that this is probably the biggest one. However, the estimate does have value in indicating the size of the errors to be expected.

The calibration is expected to depend somewhat on the changes in composition of the cosmic radiation in the atmosphere. However, a radical change is required to affect the calibration more than a percent or so. The situation at dif-

ferent times at the same altitude and latitude could not be expected to vary significantly at all. Comparisons at different latitudes would not be expected to need correction either, if measurements of 1% accuracy are being contemplated, except if an extreme situation such as that illustrated in Chapter VII B is being considered. The biggest change of the calibration is expected to be with change in altitude, because of the transition of the primary heavy particles to the lighter mesons and electrons in the atmosphere. These variations were found to be covered by the uncertainties quoted for the absolute measurement, and need not be considered in comparing altitude vs ionization curves to considerably greater accuracy.

B. Discussion of results and further experiments

A better understanding of how pressure affects ionization, how the wall changes the cosmic radiation, and how the relative ionization behaves would be desirable. An accurate analytic understanding would make possible accurate corrections, but data are lacking, and the problem is a very complicated one. More direct measurements in the line of varying the wall or the radiation are at present the only practical way to narrow the uncertainty.

The wall effect was a fairly important correction, and it was found that the important factor was the Z of the wall material. There may be also a purely surface effect, but for energies above a few ev, or at most a few hundred

ev, this should not be significant. The effect of the wall could be minimized by making its Z as close as possible to air, and also by making it thinner. The best practical material is probably aluminum, due to the sensitivity of the quartz system to organic impurity. If the wall effect in such a low Z chamber were small compared to that in an iron chamber, as expected, an accurate extrapolation could be made to no wall.

An important assumption which was made was that a penetrating particle such as a μ meson or a proton has no wall effect, if it passes through without interacting. It would be desirable to test this assumption by using, say, protons of a few hundred Mev energy from a machine. A small chamber would be most sensitive to changing its walls. It might also be possible to use the 10" chambers at mountain top levels, where most of the ionization is from mesons, although background and the electric component would make the results less clear-cut.

If a penetrating particle wall effect were important of course our estimate of the cosmic-ray wall effect is incomplete. Also $\frac{I_{air}}{I_A}$ for charged particles would depend on the size of the chamber used to measure it. The fact that the observed $\frac{I_{air}}{I_A}$ for 340-Mev protons is made in a small chamber, and agrees with an independent calculation which is independent of walls seems to indicate that there is no serious error from this cause. If 0.685 is the correct small-

chamber relative ionization, the error in the present final result caused by neglecting a proton wall effect, would be equal to the size of the neglected effect. If 0.685 is really the relative ionization for an infinite volume of gas, then the mistake in our final result would be much smaller.

It is difficult to think of an accurate ($\pm$ 1%) experiment to give the relative ionization directly. If a chamber were sent up with a plastic wall of Z about 7, and air as the gas, the measured ionization would be almost directly the ionization in the atmosphere. Unfortunately, this reintroduces the recombination eliminated by using argon at low pressure. In air, with the fields used now, recombination almost certainly would be a relatively large (a few percent) correction. The correction would depend on the same things that cause uncertainty in the argon determination. However, such an experiment would be a check on the approach described in Chapter VII.

It would also be desirable to have an accurate accounting for the difference observed between the chamber at 1 atm and a similar one at 8 atm. However, it appears that the only way this can be done is by a better understanding of the processes involved. An empirical evaluation could always be obtained by actually sending up chambers at two pressures at different latitudes. As long as they respond in the same ratio for both cosmic rays and the gamma-ray

calibration source, no error will occur in the value of ionization in air that is reported by chambers at either pressure.

Integration of the ionization vs depth curve to get the energy dissipated in ionization is an interesting calculation. This was done using the experimental curve in Fig.10 for $\lambda_m = 56^\circ$, corrected by the final average I_{air}/I_o ($+5\%$). The result was 929 Mev cm^{-2} $ster^{-1}$ sec^{-1}, assuming isotropy. This is equal to the energy flux at the top of the atmosphere, minus the energy going into neutrinos. Komori (7) has extended the detailed calculations of Rossi(6), Puppi and Dallaporta (42) for the energy lost in the atmosphere. His result, not including the neutrino energy, was 963 ± 100 Mev cm^{-2} sec^{-1} $ster^{-1}$, which is in agreement.

Assuming an average primary energy of 6 Bev, our result implies a flux of 0.15 cm^{-2} sec^{-1} $ster^{-1}$, which is also in agreement with Meredith and Van Allen (5).

The sensitivity of the calculated ionization (see Chapter III) to the percentage of heavy primaries assumed suggests that further work might be done along that line to see if a value could be obtained for the heavy primary abundance. Suppose that counters were sent aloft on the same balloon with the ionization chamber. If they were arranged to give the omni-directional flux at the same time the ionization was being measured, an average specific ionization could be obtained. The counter would not respond

to the heavy flux because, particle-wise, it is rare, but the ionization chamber does. The alpha-particle and secondary flux would be in the nature of a background, and an interpretation could be made in the framework of a Gross analysis. Absolute counter values would not be necessary; only consistent measurement of the flux in relative units. The experiment would probably be most easily done at intermediate latitudes, to minimize the effect of energy loss, but there would not seem to be any basic reason it could not be done at the pole also.

The fact that the shape of the top of the ionization vs depth curve at Bismarck changes with time, even though the geomagnetic cutoff ought to eliminate range effects, suggests that the heavy flux changes. The other, perhaps more reasonable, explanation is that slight changes in the energy spectrum of the primaries affect the production of secondaries and the perturbing effect of energy loss. Perhaps a counter and ion chamber would easily be able to distinguish the effects.

REFERENCES

1. H. Elliot, Progress in Cosmic Ray Physics, vol. 1 (North-Holland Publ. Co., Amsterdam, 1952) Chapter VIII
2. Symposium on Cosmic Rays, Univ. of Chicago, Rev. Mod. Phys., 11, 121 (1939).
3. H. V. Neher, V. Z. Peterson and E. A. Stern, Phys. Rev. 90, 655 (1953)
4. H. Carmicael and E. G. Dymond, Proc. Roy. Soc. A171, 321 (1939)
5. L. H. Meredith, J. A. Van Allen, and M. B. Gottlieb, Phys. Rev. 99, 198 (1955)
6. B. Rossi, Rev. Mod. Phys. 20, 537 (1948)
7. H. Komori, Prog. Theo. Phys. 13, 205 (1955)
8. H. V. Neher and E. A. Stern, Phys. Rev. 98, 845 (1955)
9. H. V. Neher, Phys. Rev. (to be published)
10. H. V. Neher, Rev. Sci. Instr. 24, 99 (1953)
11. B. Rossi, High Energy Particles (Prentice-Hall, Inc., New York, 1952) Chapter 8
12. M. F. Kaplon, J. H. Noon, and G. W. Racette, Phys. Rev. 96, 1408 (1954)
13. A. D. Dainton, P. H. Fowler, and D. W. Kent, Phil. Mag. 43, 729 (1952)
14. G. W. McClure, Phys. Rev. 96, 1391 (1954)

15. J. R. Winckler and K. Anderson, Phys. Rev. 93, 596 (1954)

16. J. H. Noon and M. F. Kaplon, Phys. Rev. 97, 769 (1955)

17. P. S. Frier, G. W. Anderson, J. E. Naugle, and E. P. Ney, Phys. Rev. 84, 322 (1951)

18. L. R. Davis, H. M. Caulk, and C. Y. Johnson, Phys. Rev. 91, 431 (1953)

19. B. Peters, reference 1, p. 209

20. B. Rossi, reference 11, p. 470

21. J. J. Lord, Phys. Rev. 81, 901 (1951)

22. T. Coor, Phys. Rev. 82, 478 (1951)

23. B. Rossi, reference 11, p. 469

24. R. H. Brown, U. Camerini, P. H. Fowler, W. Heitler, D. T. King, and C. F. Powell, Phil. Mag. 40, 862 (1949)

25. N. E. Bradbury, J. App. Phys. 11, 267 (1940)

26. L. B. Loeb, Basic Processes of Gaseous Electronics (Univ. of Calif. Press, Berkeley, 1955) p. 527 ff

27. E. A. Stern, Dissertation, California Institute of Technology 1955

28. R. Fuchs and W. Whaling (Unpublished)

29. W. A. Aron, B. G. Hoffman, and F. C. Williams, U.S. Atomic Energy Commission, AECU-663 (1949)

30. B. Rossi, reference 11, Chapter 5

31. J. A. Richards and L. W. Nordheim, Phys. Rev. 74, 1106 (1948)

32. P. R. Barker, Phys. Rev. 100, 860 (1955)

33. K. Greisen, Phys. Rev. 63, 323 (1943)

34. B. Rossi, reference 11, p. 29

35. C. J. Bakker and E. Segre, Phys. Rev. 81, 489 (1951)

36. E. F. Cox, Phys. Rev. 45, 503 (1934)

37. K. Kimura, P. Ishiwara, K. Yuasa, S. Yamashita, K. Miyake, and S. Kimura, J. Phys. Soc., Japan, 7, 111 (1952)

38. W. P. Jesse and J. Sadauskis, Phys. Rev. 100, 1755 (1955)

39. H. Bethe and J. Ashkin, Experimental Nuclear Physics, vol. 1, E. Segre, ed (Wiley, New York, 1953) part II.

40. E. Segre (private communication)

41. B. Rossi, reference 11, p. 489

42. G. Puppi and N. Dallaporta, reference 1, p. 381

43. F. Alder, P. Huber, and F. Metzger, Helv. Phys. Acta 20, 234 (1947)

44. W. P. Jesse and J. Sadauskis, Phys. Rev. 90, 1120 (1953)

45. R. H. Frost and C. E. Nielsen, Phys. Rev. 91, 864 (1953)

46. J. Weiss and W. Bernstein, Phys. Rev. 98, 1828 (1955)

47. J. M. Valentine, Proc. Roy. Soc. A211, 75 (1952)

48. J. Sharpe, Proc. Phys. Soc. Lond. A65, 859 (1952)

49. W. Haeberli, P. Huber, and E. Baldinger, Helv. Phys. Acta 25, 467 (1952)